國 立 交 通 大 學
機械工程學系

碩士論文

平行式油壓平台力量控制的推導與實驗

Modelling and Experiments on the Computed Force Control of

Hydraulic Parallel Machine

研 究 生：孫晏晞

指導教授：秦繼華　博士

中 華 民 國 九 十 四 年 六 月

平行式油壓平台力量控制的推導與實驗

Modelling and Experiments on the Computed Force Control of Hydraulic Parallel Machine

研究生 ：孫晏晞　　　　　　Student：Yen-His Sun

指導教授：秦繼華　　　　　　Advisor：Dr. Jih-Hua Chin

國 立 交 通 大 學

機械工程學系

碩士論文

A Thesis Submitted to Department of Mechanical Engineering

College of Engineering, National Chiao Tung University

In Partial Fulfillment of the Requirements for the degree of

Master of Science in Mechanical Engineering

June 2005

Hsinchu, Taiwan, Republic of China

中 華 民 國 九 十 四 年 六 月

平行式油壓平台力量控制的推導與實驗

研究生：孫晏晞　　　　　　指導教授：秦繼華

國立交通大學機械工程學系

論文摘要

　　平行式油壓平台(Parallel hydraulic manipulator)能夠提供巨大的能量搭載重物，並可做出許多的姿態，故傳統一般皆用於飛行模擬器上。而隨著工業的進步，對於大型工件的加工需求也越來越多，若能將平行油壓平台引進成為搭載大型工件的工具機平台，必能提升加工效率和品質；因此，如何提升油壓平台的效能和空間軌跡的追蹤能力，已為目前發展油壓平台的最大課題。本論文目的主要在於提出油壓平台的動態控制方法，並結合多軸交叉偶合預補償控制器(Multi-axis cross-coupled pre-compensation method ,MCCPM)，來求提升油壓平台的控制及軌跡追縱能力。在論文中會推導油壓平台的動態公式，找出各缸所承受力量，來做為油壓缸計算力 (Computed force)控制的依據，並以 MCCPM 來計算求得空間中軌跡誤差所需的補償量。於後面章節，提出以簡單的適應控制法並結結合切削力等外力模組，來做為往後更進一步加工機發展的控制基礎。本論文最後會經由實驗，來證明油壓平台及新控制器的工作效能及軌跡追蹤的成果。

Modelling and Experiments on the Computed Force Control of Hydraulic Parallel Machine

Student: Yen-His Sun   Advisor: Dr. Jih-Hua Chin

Department of Mechanical Engineering
National Chiao-Tung University

Abstract

Parallel hydraulic manipulator can provide large power to take heavy loading. It can do arbitrary position in workspace, so that it is generally used for flight simulation. As industrial progress, demand for cutting large and heavy work-piece is gradually increased. If hydraulic manipulator is utilized for large-scale cutting machine, then the efficiency and quality could be improved. Therefore, the key of hydraulic manipulator development is to improve the control efficacy and trajectory tracking.

In this paper, computed force control of hydraulic manipulator is presented. In addition, MCCPM, Multi-axis cross-coupled pre-compensation method, is introduced to improve the tracking ability. Dynamic formulation of hydraulic manipulator is developed for deriving the acting force on links, and computed control force; MCCPM can obtain tracking velocity to compensate trajectory error. A simplified adaptive control strategy, with external force model, is advised for the future implementation and development. Further, experimental results are presented, and also achievement of this new controller is presented.
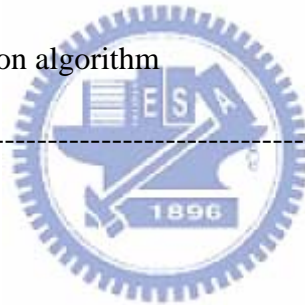
致謝

　　從這篇論文的開始到完成，遇到了相當多的困難和問題，而多虧身旁的指導老師、好友、同學、以及我敬愛的家人，能夠支持陪伴著我，讓我能夠面對這挑戰而不屈服。要感謝的人真的很多，首先、也是最重要要感謝的是我的指導教授，秦繼華教授，感謝教授不厭其煩的為我指導，無論是邏輯的構思、paper 的閱讀、論文的寫作、口試的攻防等，皆讓我的論文更加完整，也讓我更了解自己的缺陷並進而修改。我的父母總是不斷的鼓勵支持我，我的姊姊也總是能在最我最需要的時候，伸出援手給我一個擁抱；指導老師的教導讓我成長，家人的關懷讓我不至於迷失而無望，對他們的感恩之心，難以一句謝謝足以形容。此外，我的同學以及好友也是支持我走下去的關鍵，感謝實驗室的國瑋、偉倫同學，雄雄、小孔學弟，你們給了我一個很充實且充滿回憶的實驗室生活。小孩、阿海、強哥、鳥毛、鐘响等許多好友們，感謝你們始終陪著我歡笑和努力。

　　當初進研究所，我選擇了提前畢業和提前入學，就為了想縮短拿碩士的時間；但這條卻是如此難辛難走，必須犧牲許多與同學相處的時間、休息的日子等。在寫論文的過程中，我曾因不斷思考及後悔自己的行為，而感到迷失。但所幸我終究是渡過了，也許過程及結果並非如此完美，但很高興的我還是得到、學到很多，也經歷了永遠值得回味的日子。再一次的感謝所有的人，指導老師、家人、同學好友們，謝謝你們！。

<u>Contents</u>

List of figures

List of Tables

Nomenclature

q: coordinate vector with position and orientation variables z, α, β

l: link vector

P and W: platform and world frame which vector reference to

$^{W}R_p$: rotational matrix

a_i and b_i: joint vector respects to center of moving and fixed platform

L_i, l_i, and n_i: link vector, length of link, unit vector of link i

ω and α: angular velocity and acceleration

J: Jacobian matrix

F_i and M_i: vector of external force and moment, and on link i

f_i and m_i: scalar of external force and moment, and on link i

m_u and m_p: mass of link and platform

G: gravitational acceleration

$^{W}c_i$: unit vector normal to two revolute axes of universal joint

C: initial force matrix

F: vector of link reacted force

P_L: pressure of load oil

Q_L: load flow

K_{vl} and K_{pt}: valve and oil pressure coefficients

x_p : piston displacement

x_v: spool displacement

A_p : area of piston

V : total volume of cylinder chamber

β: effective bulk modulus of oil

C_l: leakage coefficient

M_t, B_p, K_c : coefficients of mass, damping, and spring

ζ and ω_h: hydraulic damping ratio, hydraulic natural frequency,

k_1 and k_2: hydraulic constants

u_1 and u_2: force and velocity command for servo valve

K_v : constant

F_c: computed force

K_p : P gain of velocity

P_a: actual position

P_e: trajectory point most close to P_a

$\boldsymbol{E}$: position tracking error vector

$\boldsymbol{E}_r$: path contour error vector

K_v and K_{iv}: PI gains of MCCPM

u and v: parameters of interpolation

σ_0 : stiffness in friction model

σ_1 : damping coefficient in friction model

σ_2: can be treated as Coulomb coefficient in friction model

F_{co} : Coulomb friction force

F_s : Stribeck force

v_s : Stribeck velocity

F_f: friction force

t_c: chip thickness

K_t , K_r , K_a : tool parameters

Y : regressor matrix

ϑ: parameter vector

V: Lyapunov candidate function

φ: deviation of parameter

CHAPTER 1

INTRODUCTION

1.0 Introduction

In general, parallel manipulator with physically closed form has advantages of high stiffness, low inertia, and large loading capacity. Parallel manipulators have been widely found in many applications, such as aircraft simulators, anti-vibrated payloads, and high-accuracy telescope. Since parallel manipulators possess higher degrees of freedom with compact mechanism, it is very suitable to be as milling or cutting machine tool. In the other side, as known, hydraulic cylinder has large power and stable dynamic performance. Therefore, parallel manipulator driven by hydraulic cylinder can provide larger loading application and milling motion, and its development becomes more and more important.

In hydraulic cylinder system, the loading force may cause effects on piston motion and make the piston unable to track trajectory accurately. A control strategy of computed force to reject force effect is proposed. With velocity control, computed force controller derives desired actuating force and compensates the valve command. Therefore, dynamic characteristics of parallel manipulator are required for obtaining the reacting forces and loads on cylinder, when platform moving.

In addition, the MCCPM is introduced to make an attempt on tracking trajectory accurately. Since, by MCCPM, trajectory error is compensated in link space, then it is unnecessary to compensate trajectory on Cartesian space. The forward kinematics is avoided, and the control efficiency is increased. Therefore, the milling ability and precision of hydraulic manipulator could be improved.

Besides, a novel control strategy is advised for such complicated system as parallel manipulator. For cutting machine, external force, like cutting force and friction, will make machine deteriorating performance. It is difficult to model these uncertain reacting forces for computed force control. Therefore, for more accurate control ability, an adaptive control, which can eliminate the problem of uncertainty of system, is developed for parallel machine tool.

The dynamic formulation of hydraulic manipulator is developed by Newton method in Chapter 2. Also, dynamic characteristic of hydraulic cylinder and computed force will be observed and discussed. In Chapter 3, the MCCPM method will be introduced; the interpolator will be used to obtain trajectory function. In Chapter 4, experimental results of trajectory tracking are exhibited and performance of controllers will be compared and discussed. Further, the conclusion and summary are drawn in Chapter 5. In Chapter 6, for future development, a simple method is advised to accomplish adaptive control algorithm, and include external reaction force, such as friction and cutting force, which will be also introduced [1][2].

1.1 Background

Hydraulic manipulator, with high load-capacity, is most used as flight simulator, which needs large power. However, it's inadequate to be as a milling machine for its poor precision. Generally, hydraulic machine has poor dynamic characteristics and unable to accurately track working trajectory. Many hydraulic researches focus on how to improve the accuracy and control performance. Concepts for computed force on hydraulic cylinder had been proposed; Lischinsky *et al* [3] computed load force with friction model and compensated it, but no dynamic is considered; Kwon *et al* [4] compensated the load and friction effect for tracking control, however they didn't apply it on parallel manipulator and system dynamic wasn't concerned. Zhow [5] developed force compensation controller for hydraulic robot, yet not for parallel manipulator. Kosuge *et al* [6] used feedback force compensation to achieve velocity control, whereas, it's very passive and unable to offer actual force information.

On the other hand, in the cutting machine, precisely tracking spatial trajectory is required; therefore, MCCPM (Multi-axis cross-couple pre-compensation) [7][8][9] algorithm is introduced to analyze the contour error and compute desired compensation for spatial trajectory. As known, in contrast to serial manipulator, link of parallel manipulator is not orthogonal, so that, the contour error should be transformed to link error and it's very time-consuming. MCCPM can directly derive compensating velocity of link and help platform track its trajectory rapidly. Here, the MCCPM algorithm is redefined and redeveloped to apply to our three-axis hydraulic manipulator [10].

Adaptive control [11]-[15] of manipulator has been very interested in many researches for recent decade, and even Dasgupta and Mruthyunjaya [16]had gathered the most control scheme and brought out ideas of parallel control strategy. It can provide robust control for coupled and nonlinear system and guarantee tracking stability. With powerful computational ability of modern computer, dynamical modeled mechanism can be calculated in time. Then, the control algorithm computes how to compensate the effects of mechanical system, including inertial, Coriolis, gravity, friction and other force. Adaptive control with cross-coupled pre-compensation has been discussed in Chin and Tsai's [9], yet he implemented it on robotic manipulator (PUMA 560). In the future, adaptive control scheme can be utilized on hydraulic manipulator, and consider reacted friction and milling force on machine tool to realize its practicability.

CHAPTER 2

KINEMATICS AND DYNAMICS ANALYSES
OF HYDRAULIC MANIPULATOR

2.0 Introduction

Our hydraulic parallel machine which has three degrees-of-freedom is composed of three hydraulic cylinders and one moving platform. Each cylinder is connected with universal joints in their both ends, and the platform is bounded on the up-end of piston. The position and orientation of the platform is determined by lengths of cylinders. Generally, inverse kinematics is used to derive how long the cylinders should lengthen and make cylinders reach desired position and orientation of platform. Our main purpose is to control the three cylinders to track desired trajectories. For controlling the three hydraulic cylinders of machine more efficiently, dynamic model must be concerned. Inverse dynamics is utilized to derive demand forces of cylinders when trajectory proceeding. So, the computed force can provide the command of control cylinder. Since dynamic formulations of Parallel Platform are quite numerically complicated, many mathematical methods, for, Lagrange [17], and principal virtual work method [18][19], have been formulated for solving this dynamics problem. In this paper Newton-Euler formulation [20][21][22] is introduced to derive dynamics, and the dynamic of hydraulic will be discussed, too.

2.1 Coordinate system

The moving platform of hydraulic manipulator possesses three degrees-of-freedom which can be written a coordinate vector q with position and orientation variables [20]

$$q = (z, \alpha, \beta)^T \tag{2.1}$$

z are Cartesian vector along to Z-axis, and α, β are Euler angle representation. The link space is consisted of 3-variables

$$l = \begin{bmatrix} l_1 & l_2 & l_3 \end{bmatrix}^T \tag{2.2}$$
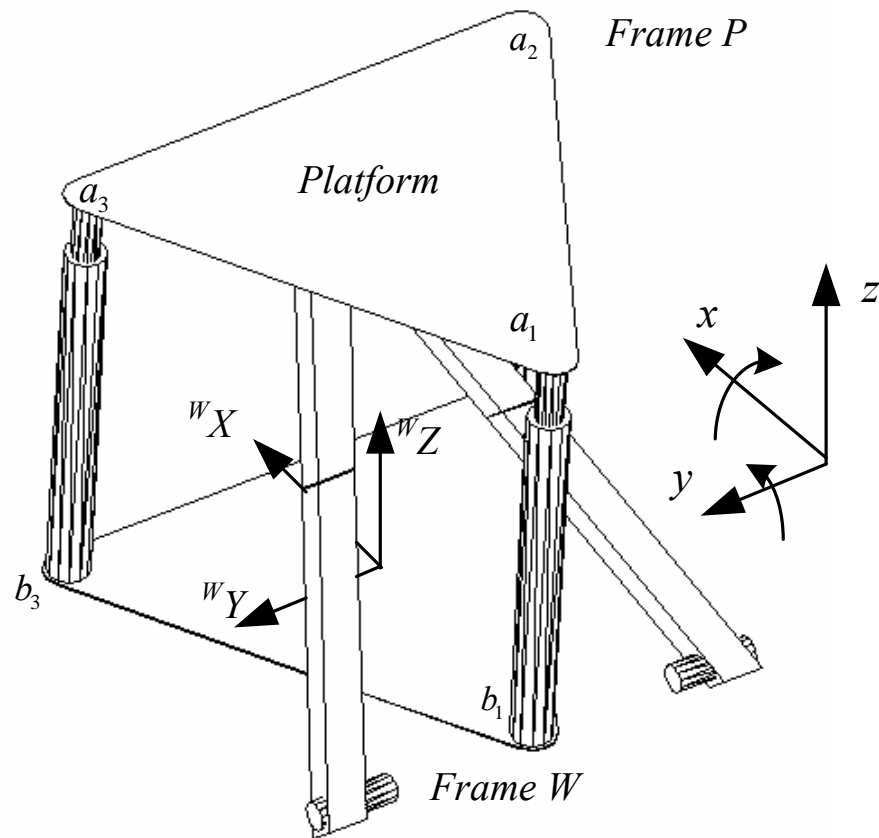
Fig. 2.1. (a) Hydraulic manipulator

Fig. 2.1. (b) Hydraulic motion platform

Hydraulic manipulator is as shown in Fig. 2.1 (a) and (b).A triangular support is connected to the center of platform with a pair of revolute joints; therefore it can eliminates residual degrees of freedom when singularity of equivalent lengths occurring. Whereas, the triangular support would constrain mobility of manipulator and reduce its workspace, and it drives the platform respect to X axis. As parallel manipulator, three hydraulic cylinders' lengths specify the pose of platform. And operator reaches the desired pose by adjusting lengths of cylinders. In Fig. 2.2, the frame **W** is world fixed frame; the frames **P** are reference frames which are attached to the moving platform, as seen in Fig. 2. The origin of coordinates **P** and **W** is assumed to be located on the mass center of platform and base. At initial position, coordinate frame **P** reference to frame **W** are represented

$$^{W}\boldsymbol{P} = \begin{pmatrix} 0 & 0 & z \end{pmatrix}^{T} \tag{2.3}$$

The other coordinate frame **P** with orientation rotation reference to frame **W** can be written as [20]

$$^{W}\boldsymbol{P} = \begin{pmatrix} 0 & 0 & z_{P} \end{pmatrix}^{T} + {^{W}R_{P}} {^{P}\boldsymbol{P}} \tag{2.4}$$
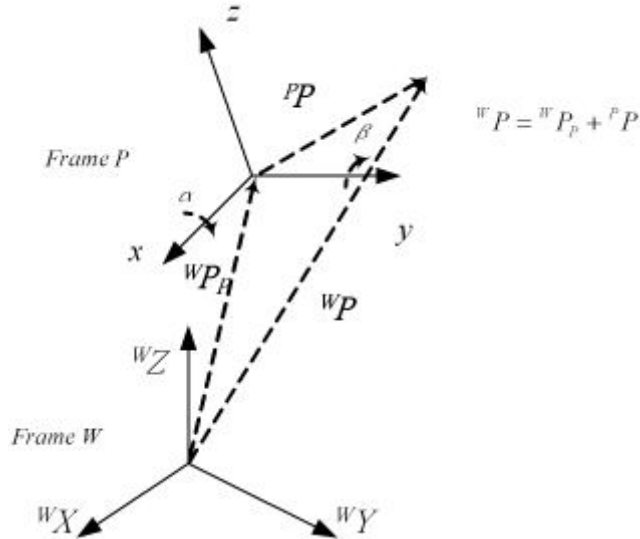
Fig. 2.2. Coordinates transformation

$^{W}R_{p}$ is rotational matrix which is consisted of rotation about x, y -axes:

Rotation α about the X-axis of the moving coordinate **P**

$$R(x, \alpha) = \begin{bmatrix} 1 & 0 & 0 \\ 0 & c\alpha & -s\alpha \\ 0 & s\alpha & c\alpha \end{bmatrix} \qquad (2.5)$$

Rotation β about the Y-axis of the moving coordinate **P**

$$R(y, \beta) = \begin{bmatrix} c\beta & 0 & s\beta \\ 0 & 1 & 0 \\ -s\beta & 0 & c\beta \end{bmatrix} \qquad (2.6)$$

Since the angular rotation about the Z-axis of the moving coordinate **P** is locked, then the transformation matrix is as element matrix

$$R(z, \gamma) = \begin{bmatrix} 1 & 0 & 0 \\ 0 & 1 & 0 \\ 0 & 0 & 1 \end{bmatrix} \qquad (2.7)$$

The rotational matrix $^{W}R_{p}$ is obtained by multiplying the three rotation matrix

$$^{W}R_{P} = R(z, \gamma)R(y, \beta)R(x, \alpha) = \begin{bmatrix} c\beta & s\beta s\alpha & s\beta c\alpha \\ 0 & c\alpha & -s\alpha \\ -s\beta & c\beta s\alpha & c\beta c\alpha \end{bmatrix} \qquad (2.8)$$

,where **c** and **s** denote *cosine* and *sine* function.

2.2 Inverse kinematics

2.2.1. Inverse position kinematics

In Figure 2.1 (a), the points a_i i=1,2,3 on the moving platform are joint locations. The a_i vector reference to frame **P** can be written as [20]

$$^{W}a_i = {^{W}x_p} + {^{W}R_P}\, {^{P}a_i} \quad , \quad {^{W}x_p} = \begin{bmatrix} 0,0,z \end{bmatrix}^{T} \tag{2.9}$$

$^{P}a_i$ is a vector a_i with reference to frame **P**. Once the a_i is obtained, the limb vector L_i can be expressed as

$$^{W}L_i = {^{W}a_i} - {^{W}b_i} \tag{2.10}$$

The limb length l_i which is the distance vector L_i can be computed as

$$l_i = \sqrt{L_i \cdot L_i} \tag{2.11}$$

Thus, the link space can be written as

$$l = \begin{bmatrix} l_1 & l_2 & l_3 \end{bmatrix}^{T} = \begin{bmatrix} \|L_1\| & \|L_2\| & \|L_3\| \end{bmatrix}^{T} \tag{2.12}$$

and unit vector can also be obtained [20]

$$^{W}n_i = \frac{^{W}L_i}{l_i} \tag{2.13}$$
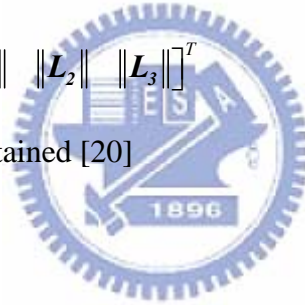
2.2.2. Inverse velocity kinematics

The velocity of a_i is determined by taking time differentiating of equation (2.9)

$$^W\dot{a}_i = {}^W\dot{x}_p + \omega_P \times {}^WR_P{}^Pa_i \ , \ \ {}^W\dot{x}_p = [0,0,\dot{z}]^T \text{ and } \omega_P = \begin{bmatrix} \dot{\alpha} & \dot{\beta} & 0 \end{bmatrix}^T \ (2.14)$$

Then, the limb velocity is projection of velocity vector a_i on the limb vector n_i

$$\dot{l}_i = {}^W\dot{a}_i \cdot {}^Wn_i = {}^W\dot{x}_p \cdot {}^Wn_i + \omega_P \cdot \left({}^WR_P{}^Pa_i \times {}^Wn_i\right) \tag{2.15}$$

From above Equation (2.15), an inverse *Jacobian* matrix can be found [20]

$$\dot{l} = J^{-1}{}^W\dot{q} \ , \ \ {}^W\dot{q} = \begin{bmatrix} \dot{z} \\ \dot{\alpha} \\ \dot{\beta} \end{bmatrix} \tag{2.16}$$

where

$$J^{-1} = \begin{bmatrix} n_{1,z}{}^T & \left({}^WR_P{}^Pa_1 \times {}^Wn_1\right)_{x,y}{}^T \\ \vdots & \vdots \\ n_{3,z}{}^T & \left({}^WR_P{}^Pa_3 \times {}^Wn_3\right)_{x,y}{}^T \end{bmatrix}, \text{ subscript } x, y, z \tag{2.17}$$

The singular position will occur when det(J)=0, which may appear in the workspace. In this case, the trajectory planning needs to avoid the singularities place for precise work.

2.2.3. Inverse acceleration kinematics

The acceleration of a_i is determined by taking time differentiating of Equation (2.14) [20]

$$^W\ddot{a}_i = {}^W\ddot{x}_p + \alpha_P \times {}^WR_P{}^Pa_i + \omega_p \times \left(\omega_P \times {}^WR_P{}^Pa_i\right) \ , \ \ {}^W\ddot{x}_p = [0,0,\ddot{z}]^T \ (2.18)$$

Therefore, the $\ddot{l}_i$ can be easily found by differentiating Equation (2.15) respecting to time

$$\ddot{l}_i = {}^W\ddot{a}_i \cdot {}^Wn_i - l_i\left(\omega_i \times \left(\omega_i \times {}^W\dot{n}_i\right)\right) \cdot {}^Wn_i \tag{2.19}$$

where

$$\omega_i = \left({}^Wn_i \times {}^W\dot{a}_i\right)/l_i \tag{2.20}$$

ω_i is the angular velocity of limb and the angular acceleration of limb α_i also can be

obtained

$$\boldsymbol{\alpha}_i = \left({}^W\boldsymbol{n}_i \times {}^W\ddot{\boldsymbol{a}}_i - 2\dot{l}_i\boldsymbol{\omega}_i \right)/l_i \tag{2.21}$$

The angular velocity and acceleration variables $\boldsymbol{\omega}_i$ and $\boldsymbol{\alpha}_i$ are used to compute the link dynamics.

2.3 Inverse dynamics

2.3.1 Dynamics equation

The dynamics of parallel manipulators is complicated and highly nonlinear. There exist several approaches to build the dynamics, such as Newton-Euler formulation, Lagrangian formulation, and the principle of virtual work method. In this paper, Newton-Euler formulation is used to develop the dynamics equations of the system [23].

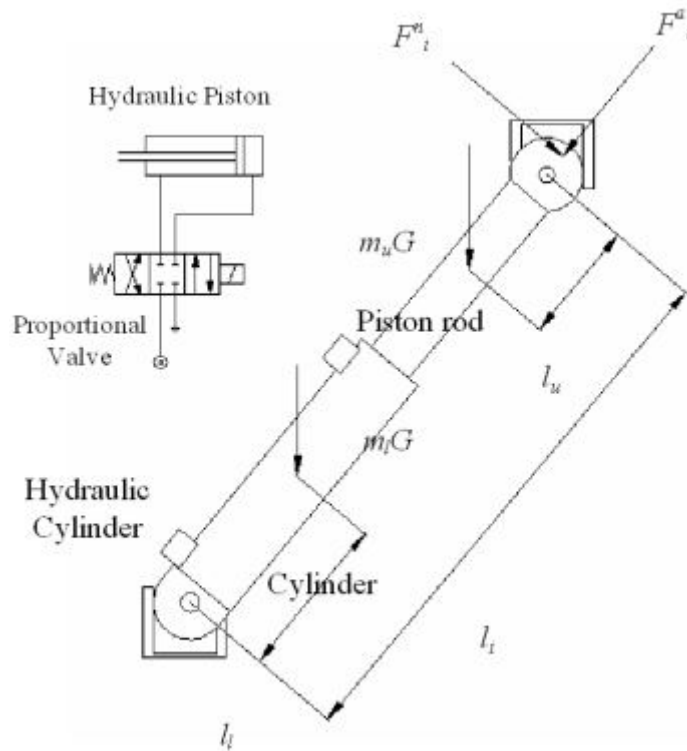Fig. 2.3. Forces components and length expressions on link i

The links of the parallel platform are driven by hydraulic piston, which is controlled by servo valve. The link's upper rod is a moving piston, which is attached to platform with universal joint. The piston is pushed up by hydraulically power pump, besides lower cylinder is stationary part attached to fixed base with universal joint.

The accelerations of the two parts can be derived as [23]

$$^{W}\boldsymbol{a}_{iu} = (l_i - l_u)\boldsymbol{\omega}_i \times (\boldsymbol{\omega}_i \times ^{W}\boldsymbol{n}_i) + (l_i - l_u)\boldsymbol{\alpha}_i \times ^{W}\boldsymbol{n}_i + 2\boldsymbol{\omega}_i \times \dot{l}_i^{\ W}\boldsymbol{n}_i + \ddot{l}_i^{\ W}\boldsymbol{n}_i \quad (2.22)$$

$$^{W}\boldsymbol{a}_{il} = l_l\boldsymbol{\omega}_i \times (\boldsymbol{\omega}_i \times ^{W}\boldsymbol{n}_i) + l_l\boldsymbol{\alpha}_i \times ^{W}\boldsymbol{n}_i \quad (2.23)$$

where subscript u and l denote upper and lower part of link.

For developing the dynamic of hydraulic manipulator, the force interacted between links and platform is necessary. As seen in Fig 2.3., $\boldsymbol{F}_i^a$ and $\boldsymbol{F}_i^n$ are force acted on the spherical joint with platform in frame W: $\boldsymbol{F}_i^a$ is force component directed to limb axis, and $\boldsymbol{F}_i^n$ is force component normal to $\boldsymbol{F}_i^a$. Therefore, the external force on link $\boldsymbol{F}_i$ is the summation of $\boldsymbol{F}_i^a$ and $\boldsymbol{F}_i^n$.

$$\boldsymbol{F}_i = \boldsymbol{F}_i^a + \boldsymbol{F}_i^n \quad (2.24)$$

Moment of link by external force is equivalent to inertia moment [23]

$$m_u(l_i - l_u)^W\boldsymbol{n}_i \times \boldsymbol{G} + m_l l_l^{\ W}\boldsymbol{n}_i \times \boldsymbol{G} + l_i^{\ W}\boldsymbol{n}_i \times \boldsymbol{F}_i^n + ^{W}\boldsymbol{M}_i$$
$$= (I_u + I_l)\boldsymbol{\alpha}_i - (I_u + I_l)\boldsymbol{\omega}_i \times \boldsymbol{\omega}_i + m_u(l_i - l_u)^W\boldsymbol{n}_i \times ^{W}\boldsymbol{a}_{iu} + m_l l_l^{\ W}\boldsymbol{n}_i \times ^{W}\boldsymbol{a}_{il}$$

$$(2.25)$$

where m_u and m_l are mass of rod and cylinder. $\boldsymbol{G}$ is gravitational acceleration, I_u, I_l are inertia moment of mass of rod and cylinder respect to frame **W**. M_i is reaction moment, which is transmitted from universal joint, and written as

$$^{W}\boldsymbol{M}_i = m_i^{\ W}\boldsymbol{c}_i \quad (2.26)$$

where $^{W}\boldsymbol{c}_i$ is a unit vector normal to two revolute axes of universal joint, and m_i is magnitude of this reaction moment. Here hydraulic piston and cylinder are assumed as asymmetric rigid bodies, like cylindrical rod.

$$^{W}\boldsymbol{c}_i = \frac{^{W}\boldsymbol{b}_i}{\left\|^{W}\boldsymbol{b}_i\right\|} \times \left(\frac{^{W}\boldsymbol{b}_i \times ^{W}\boldsymbol{n}_i}{\left\|^{W}\boldsymbol{b}_i \times ^{W}\boldsymbol{n}_i\right\|}\right) \quad (2.27)$$

In order to make equation (2.25) compact, new algebraic variable N_i is assumed

$$^{W}\boldsymbol{M}_i + l_i^{\ W}\boldsymbol{n}_i \times \boldsymbol{F}_i^n = m_i^{\ W}\boldsymbol{c}_i + l_i^{\ W}\boldsymbol{n}_i \times \boldsymbol{F}_i^n = ^{W}\boldsymbol{N}_i \quad (2.28)$$

where N_i is from [23]

$$^W N_i = -m_u(l_i - l_u)\, ^W n_i \times G - m_l l_l\, ^W n_i \times G + (I_u + I_l)\alpha_i$$
$$- (I_u + I_l)\omega_i \times \omega_i + m_u\left(l_i - l_u\right)\, ^W n_i \times\, ^W a_{iu} + m_l l_l\, ^W n_i \times\, ^W a_{il} \qquad (2.29)$$

Therefore, m_i can be obtained by taking dot product of Equation (2.29) with $^W n_i$ and presented

$$m_i = \frac{\left(^W N_i \cdot\, ^W n_i\right)}{\left(^W c_i \cdot\, ^W n_i\right)} \qquad (2.30)$$

Determined m_i is introduced to equation (2.28) and normal force can be derived F_i^n.

$$F_i^n = \frac{\left(^W N_i \times\, ^W n_i - m_i\, ^W c_i \times\, ^W n_i\right)}{l_i} \qquad (2.31)$$

For generalization, the entire force and moment, acting on platform respect to Frame **W,** are consisted of force and moment from links and can be evaluated as [23]

$$m_p\, ^W \ddot{x}_P - \sum_{i=1}^{3} f_i^a\, ^W n_i - \sum_{i=1}^{3} F_i^n = m_p G \qquad (2.32)$$

where $F_i^a = f_i^a\, ^W n_i$, and

$$-\sum_{i=1}^{3} f_i^a\, ^W R_P\, ^P a_i \times\, ^W n_i - \sum_{i=1}^{3} ^W R_P\, ^P a_i \times F_i^n - \sum_{i=1}^{3} M_i = I_P \alpha_P - I_P \omega_P \times \omega_P \quad (2.33)$$

where m_p and I_p are mass and inertia moment of platform. Hence, axial force of struts can be funded from above two force equilibrium equations (2.32) and (2.33), which can be expressed as

$$m_p\, ^W \ddot{x}_P - m_p G - \sum_{i=1}^{3} F_i^n = \sum_{i=1}^{3} f_i^a\, ^W n_i \qquad (2.34)$$

and

$$-I_P \alpha_P + I_P \omega_P \times \omega_P - \sum_{i=1}^{3} ^W R_P\, ^P a_i \times F_i^n - \sum_{i=1}^{3} M_i = \sum_{i=1}^{3} f_i^a\, ^W R_P\, ^P a_i \times\, ^W n_i \quad (2.35)$$

Because this hydraulic platform moves on Z, α, β, there are only motions about these directions that need to be considered. Then, an inverse Jacobian matrix is found to replace equation (2.34) and (2.35) as

$$\begin{bmatrix} {}^W\boldsymbol{n}_{1,z} & \cdots & {}^W\boldsymbol{n}_{3,z} \\ \left({}^W R_P {}^P\boldsymbol{a}_1 \times {}^W\boldsymbol{n}_1\right)_{x,y} & \cdots & \left({}^W R_P {}^P\boldsymbol{a}_3 \times {}^W\boldsymbol{n}_3\right)_{x,y} \end{bmatrix} \begin{pmatrix} f_1^a \\ \vdots \\ f_3^a \end{pmatrix} = C \qquad (2.36)$$

where

$$C = \begin{bmatrix} \left(m_p {}^W\ddot{\boldsymbol{x}}_P - m_p \boldsymbol{G} - \sum_{i=1}^{3} \boldsymbol{F}_i^n \right)_z \\ \left(-I_P \boldsymbol{\alpha}_P + I_P \boldsymbol{\omega}_P \times \boldsymbol{\omega}_P - \sum_{i=1}^{3} {}^W R_P {}^P\boldsymbol{a}_i \times \boldsymbol{F}_i^n - \sum_{i=1}^{3} \boldsymbol{M}_i \right)_{x,y} \end{bmatrix} \qquad (2.37)$$

$$J^{-T} = \begin{bmatrix} {}^W\boldsymbol{n}_{1,z} & \cdots & {}^W\boldsymbol{n}_{3,z} \\ \left({}^W R_P {}^P\boldsymbol{a}_1 \times {}^W\boldsymbol{n}_1\right)_{x,y} & \cdots & \left({}^W R_P {}^P\boldsymbol{a}_3 \times {}^W\boldsymbol{n}_3\right)_{x,y} \end{bmatrix} \qquad (2.38)$$

Than the axial force f_i^a of limb i, i=1, 2, 3 , can be obtained by multiplying Jocobian matrix

$$\begin{pmatrix} f_1^a \\ \vdots \\ f_3^a \end{pmatrix} = J^T C \qquad (2.39)$$

The force f_i of link i, i=1, 2, 3 , actuated by piston is determined by summing reaction force along to axial direction and expressed as

$$f_i = m_u \boldsymbol{a}_{iu} \cdot {}^W\boldsymbol{n}_i - f_i^a - m_u \boldsymbol{G} \cdot {}^W\boldsymbol{n}_i \qquad (2.40)$$

From above equations, actuation force of links $\boldsymbol{F}$ can be obtained as

$$\boldsymbol{F} = \begin{pmatrix} f_1 \\ \vdots \\ f_3 \end{pmatrix} = \begin{pmatrix} m_u \left(\boldsymbol{a}_{1u} - \boldsymbol{G} \right) \cdot \boldsymbol{n}_1 \\ \vdots \\ m_u \left(\boldsymbol{a}_{3u} - \boldsymbol{G} \right) \cdot \boldsymbol{n}_3 \end{pmatrix} - J^T C \qquad (2.41)$$

Therefore, an inverse dynamic program for calculating link force with equations (2.1)-(2.41) can be written on computer. It is introduced in Section 2.3.2. In our system, hydraulic piston is independently controlled for tracking in joint space. Thus, the dynamical formulation of manipulator is developed for computing the force, so as

to reject force disturbance and control piston as general linear system. Control strategy of hydraulic piston will be discussed in Section 2.6.

2.3.2 Dynamics programming

With derivation of kinematics and dynamics equations (2.1) – (2.41), a PC is utilized to compute the force for parallel manipulator as it process some trajectories

$$\boldsymbol{F} = Dynamics\left(q, \dot{q}, \ddot{q}\right) \tag{2.42}$$

Here, the results of program simulation are presented. And its material data and design dimension of hydraulic machine are shown in Table. 2.1-2.2.

Table 2.1. Designate data

Mass Inertia (kg)		Moment Inertia (kg-m^2)	
Upper Limb	5	I^{upper}_{axis}	5
Lower Limb	5	I^{lower}_{axis}	7
Motion platform	8.5	$I^{platform}$	0.7938
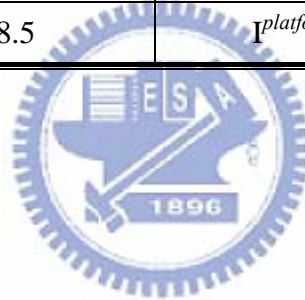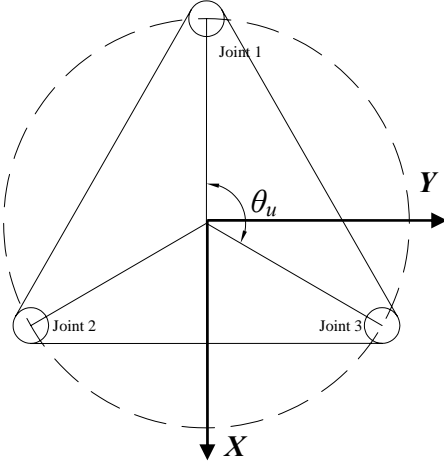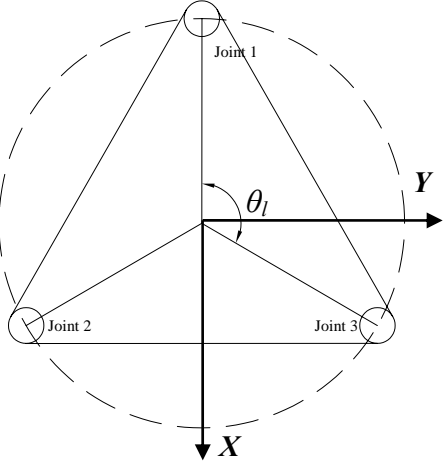
Table 2.2. Platform and Base layouts

Upper platform	***Lower Bases***
φ_u=800 mm	φ_l=800 mm
θ_u=120°	θ_l=120°

Link motion and force are simulated by computer and presented as Fig. 2.4 and 2.5. Below figures are divided into cylinder displacement that are computed from equations (2.1)-(2.12), and actuating force computed from equations (2.22)-(2.41) respectively. Two trajectories are tested and their motion function are

Trajectory 1: $Z(t) = 650$, $\alpha(t) = \dfrac{\pi}{15}\cos(1.2\pi t)$, $\beta(t) = \dfrac{\pi}{15}\sin(1.2\pi t)$

Trajectory 2: $Z(t) = 600 + 10t$, $\alpha(t) = 0$, $\beta(t) = \dfrac{\pi}{18}\sin(0.4\pi t)$

Trajectory 1: $Z(t) = 650$, $\alpha(t) = \dfrac{\pi}{15}\cos(1.2\pi t)$, $\beta(t) = \dfrac{\pi}{15}\sin(1.2\pi t)$
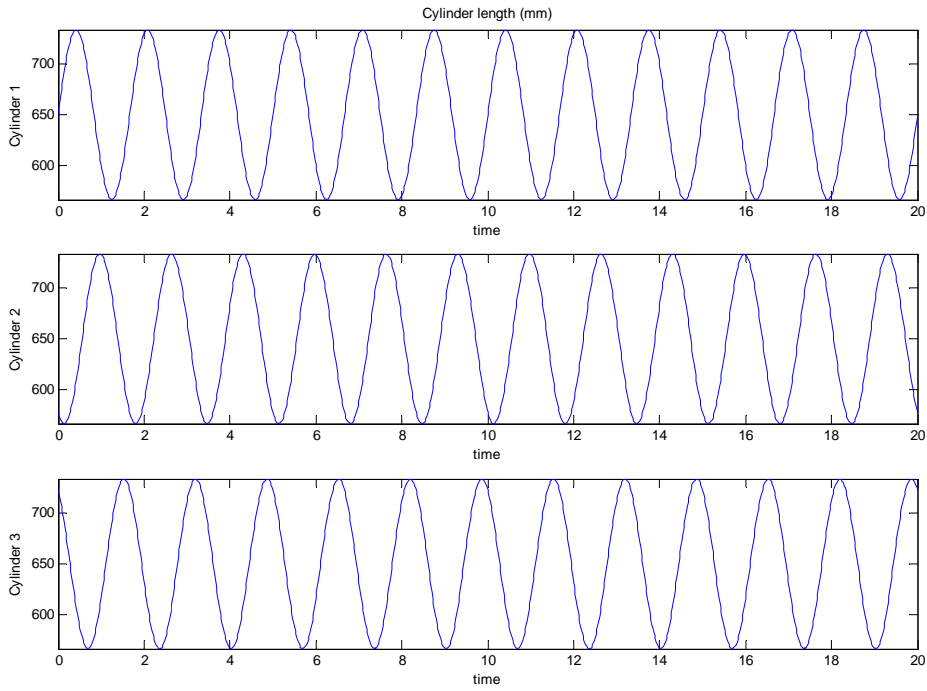
Fig. 2.4. (a) Displacement of cylinder from equation (2.12)
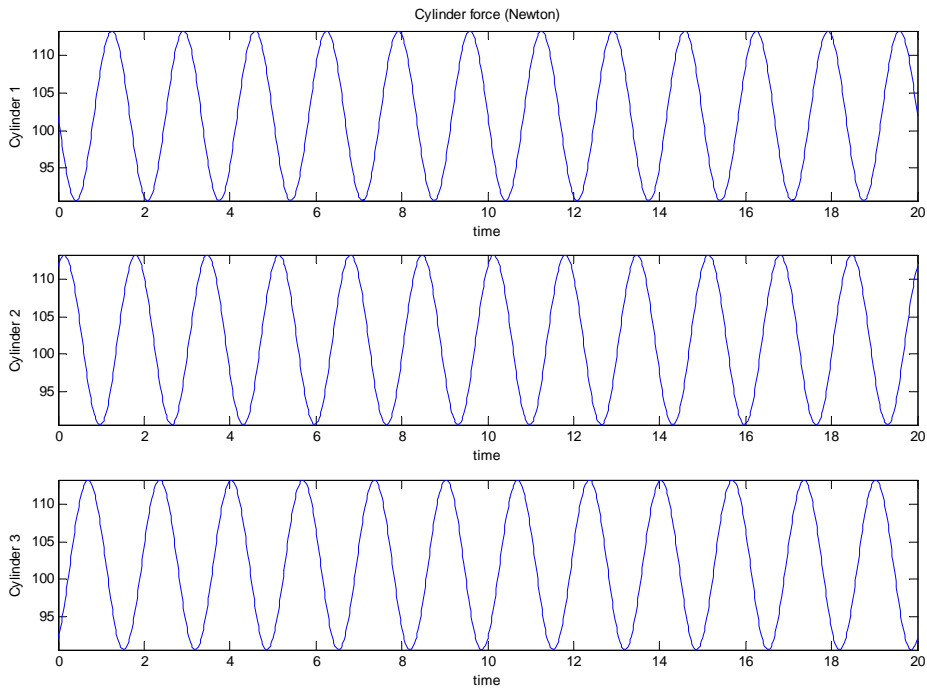
Fig. 2.4. (b) Computed force from equation (2.41)

Trajectory 2: $Z(t) = 600 + 10t,\ \alpha(t) = 0,\ \beta(t) = \dfrac{\pi}{18}\sin(0.4\pi t)$
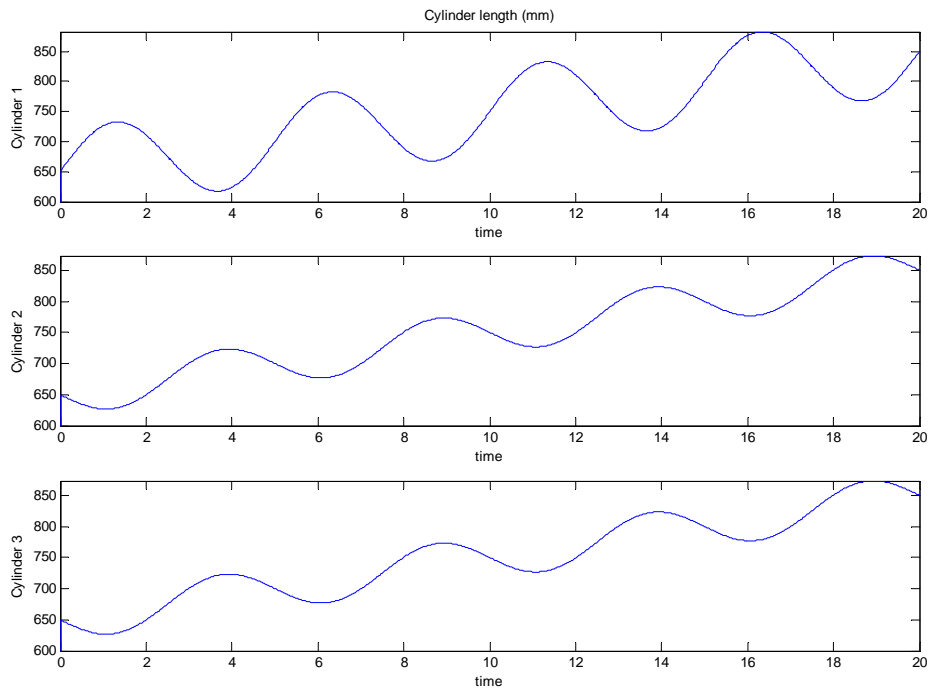
Fig. 2.5. (a) Displacement of cylinder from equation (2.12)
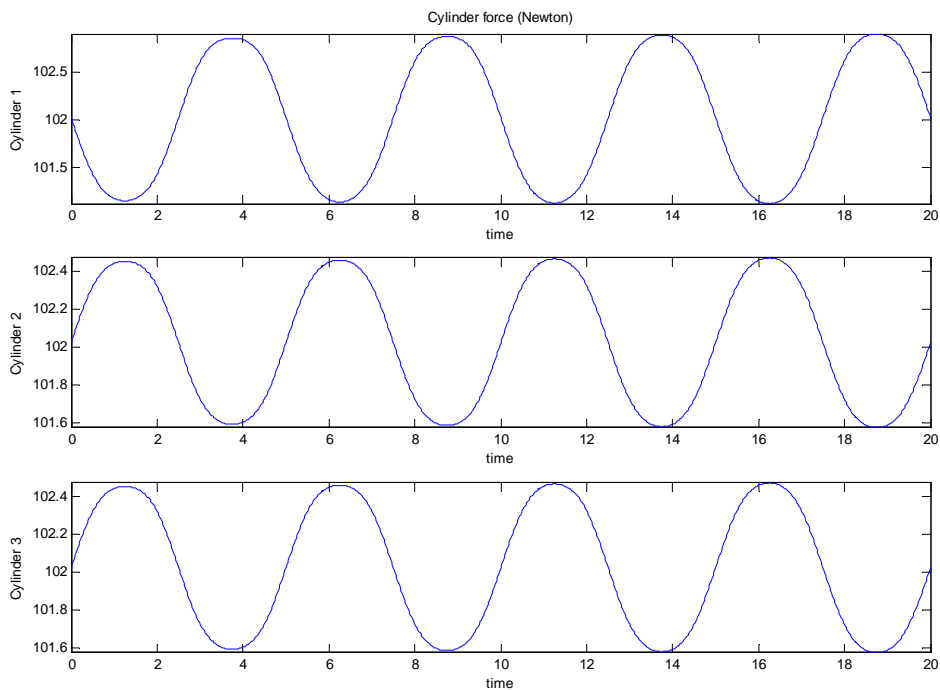
Fig. 2.5. (b) Computed force from equation (2.41)

As inverse dynamics is derived, the force computation can be carried out. In figures, the joints receive larger force when cylinders are decreasing length. It is quite reasonable that joint takes more reacted force when downward acceleration, composed of gravity and downward acceleration, increases. The result can help us understand the system model and make correct force command when cylinders are controlled. Above two trajectories will be introduced to trajectory experiment in Chapter 4.

Nevertheless, the inverse dynamics is in an ideal situation and evaluated without considering the friction and some environment effects. For further development, adaptive controller, simplifying dynamical formulation, is implemented to estimate the friction parameter and increase the robustness of the system. The implementation of adaptive controlling will be discussed in Chapter 4.

2.4 Forward kinematics

Generally, link lengths are the only information obtained, so it's necessary to derive forward kinematics to find the Cartesian coordinate vector of platform. However, the same condition of link lengths may have many different position of platform, the forward kinematics is more difficult to calculate. There are several approaches to find the forward kinematics; Raghavan and Tsai [20] had solved the forward kinematics with 40 possible solutions. Nevertheless, only one solution is consistent with actual position of platform. Therefore, Chin and Peng [25] proposed numerically iterative method, based on the Newton-Raphson method, to find out the approximate solution.

For solving the problem, a closed-loop function $FL_i(q)$ is defined as [25]

$$FL(\boldsymbol{q}) = \sum_{i=1}^{3} \left(L_i(q)^2 - l_i^2 \right) = 0 \qquad (2.43)$$

where $\boldsymbol{i}$ denotes limb number and $L_i(q)$ is link length function, which determines the link length by inverse kinematics with coordinate vector $\boldsymbol{q}$. Thus, Taylor expansion of the function is taken

$$FL(\boldsymbol{q})|_{q=q_{(n)}} = FL(\boldsymbol{q})|_{q=q_{(n-1)}} + \boldsymbol{\Delta q} \cdot \left(\frac{\partial FL}{\partial q}|_{q=q_{(n-1)}} \right) \qquad (2.44)$$

where subscript n means iterative count. So, $\dfrac{\partial FL_i}{\partial q}$ is derived as

$$\frac{\partial FL(\boldsymbol{q})}{\partial \boldsymbol{q}}|_{q=q_{(n-1)}} = \begin{pmatrix} \dfrac{\partial FL_1(\boldsymbol{q})}{\partial z} & \dfrac{\partial FL_1(\boldsymbol{q})}{\partial \alpha} & \dfrac{\partial FL_1(\boldsymbol{q})}{\partial \beta} \\ \vdots & & \vdots \\ \dfrac{\partial FL_3(\boldsymbol{q})}{\partial z} & \cdots & \dfrac{\partial FL_3(\boldsymbol{q})}{\partial \beta} \end{pmatrix}|_{q=q_{(n-1)}} \qquad (2.45)$$

As [20], $\dfrac{\partial FL_i}{\partial q}$ is the same to Jacobian matrix $\boldsymbol{J^1}$. As a result, the desired vector $\boldsymbol{q}_{(n)}$

can be easily computed as

$$\boldsymbol{q}_{(n)} = \boldsymbol{q}_{(n-1)} + J \cdot \left(FL(\boldsymbol{q})|_{\boldsymbol{q}=\boldsymbol{q}_{(n)}} - FL(\boldsymbol{q})|_{\boldsymbol{q}=\boldsymbol{q}_{(n-1)}} \right) \tag{2.46}$$

2.4.1 Iterative step of Newton-Raphson method

There are several iterative steps as followings

Step 1. Set vector $\boldsymbol{q}$ and link length $\boldsymbol{l}$ as initial position and determine function FL

Step 2. Compute deviation vector Δq by derive $J \cdot \Delta F(q)$

Step 3. Add Δq to $\boldsymbol{q}$, $q_{(n)} = q_{(n-1)} + \Delta q$, and determine new function $FL_{(n)}$

Step 4. Repeat Step 2 to Step3, until the Δq is smaller than acceptable error, and $\boldsymbol{q}$ is approximate to realistic position of platform.

Tsai [20] proposed that in addition to boundary, the singularity is occurred when Jacobian matrix of manipulator is singular, and then analytical solution will diverge. In hydraulic manipulator with triangular support, the singularity surface is rejected within workspace. Thus any trajectory in efficacious workspace is allowed and the singular of Jacobian matrix does not exist.
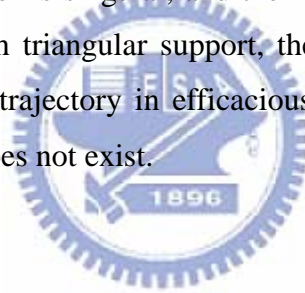
2.5 Forward dynamics

In contrast to inverse dynamics, forward dynamics equations derive the position, velocity, and acceleration condition from information of link force. As inverse dynamics, several methods [22],[21] are proposed to derive forward dynamic, such as Newton-Euler method, principle of virtual work, and Lagrangian formulation. Forward dynamics is commonly used for simulating motion process of manipulator. Here a simple dynamics formulation is funded, which can obtain manipulator information with link force input. [26]

$$F = M(q_a)\ddot{q} + N(q_a,\dot{q}_a) + G(q_a) \qquad (2.47)$$

where M is inertia mass matrix, N is vector of centrifugal/Coriolis force, and G is vector of gravitational force. The equations of inverse dynamics are derived and programmed, where program is as a dynamics function with dynamical parameters input

$$F = Dynamics(q,\dot{q},\ddot{q}) \qquad (2.48)$$

As known, the analytical solutions of acceleration can be computed by multiplying inverse mass matrix $M(q_a)$ [26]

$$\ddot{q} = M^{-1}(q_a)(F - F') \qquad (2.49)$$

where

$$F'(q_a,\dot{q}_a) = N(q_a,\dot{q}_a) + G(q_a) \qquad (2.50)$$

The F' program is a subroutine of dynamics program, and it is for computing coupling force effect, which is obtained by dynamics function given $\ddot{q} = 0$ input.

$$F' = Dynamics(q,\dot{q},\ddot{q} = 0) \qquad (2.51)$$

Then, for deriving mass matrix $M(q_a)$, dynamics function is re-executed with giving $q = 0, \dot{q} = 0$ and gravitational G=0 input. And further column of matrix $M(q_a)$ is computed by input $\ddot{q}_i = 1$ and $\ddot{q}_j = 0$ for $i \neq j$

$$M_i(q) = \begin{bmatrix} \vdots & m_i(q) & \vdots \end{bmatrix} = Dynamics(q = 0, \dot{q} = 0, \ddot{q}_i)|_{G=0} \qquad (2.52)$$

Hence, mass matrix can be obtained, and the analytical solution can be obtained. Thus, other velocity, position term are derived by numerically integration. The computer simulator process is similar to [26], and shown in Fig. 2.6
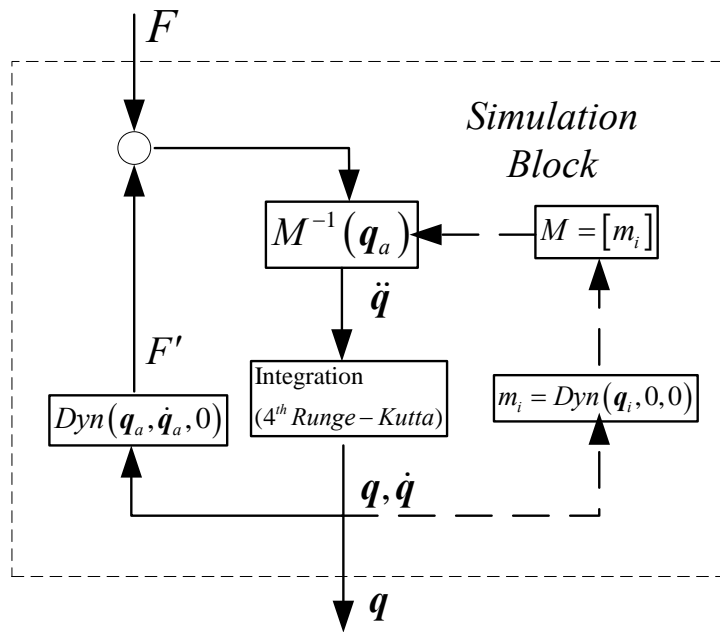
Fig. 2.6. Simulation block diagram

2.6 Dynamics of hydraulic piston and computed force control

The links of manipulator are hydraulic power element, which are combinations of servo valve and piston. In order to improve the manipulator precision, the hydraulic cylinder must be controlled more accurately. The research of hydraulic has been developed for a long time, and many control schemes for improving hydraulic tracking were investigated and proposed, for instance, conventional PID controller [27] or the adaptive control of hydraulic cylinder [28]. Intuitionally, the load force may have negative contribution to piston, so the load force effect on hydraulic cylinder is concerned about in many papers. When the load is much smaller than allowable range the cylinder can hold, the load force, certainly, has slight effect on hydraulic. But for larger scale of load, large negative effect will dominate the performance of cylinder [4]. Therefore, to reject force effect and improve the performance of cylinder, computed force is proposed for our control system.

The servo valves of hydraulic manipulator are commanded by PC base, and feedback signal of piston length are read by potentiometers. The piston is pushed by oil pressure, and than its motion is involved with spool displacement, which can adjust the oil pressure.
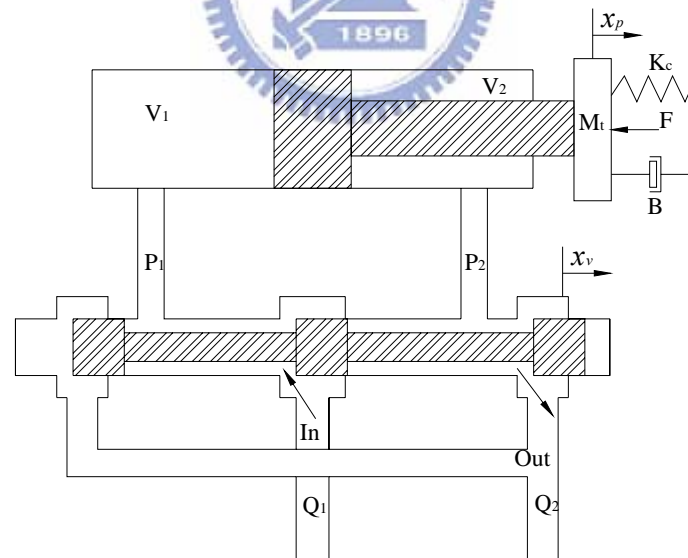
Fig. 2.7. Servo-valve and cylinder system

Merritt [4] had proposed a flow equations of hydraulic piston is related to spool displacement x_v and load pressure P_L

$$Q_L = \frac{(Q_1 + Q_2)}{2} = K_v x_v - K_p P_L \tag{2.53}$$

, where Q_L is load flow which is seen in Fig. 2.7, K_{vl} and K_{pt} coefficients, and

$P_L = \frac{(P_1 - P_2)}{2}$. Also, the cylinder continuity equation is approximated by [4]

$$Q_L = A_p \dot{x}_p + \frac{V}{4\beta} \dot{P}_L + C_l P_L \tag{2.54}$$

, where x_p is piston displacement, A_p area of piston, V total volume of cylinder chamber, β effective bulk modulus of oil, and C_l leakage coefficient. Because the oil is compressibility flow, then term $\dfrac{V}{4\beta} \dot{P}_L$ can be ignored, and equation (2.54) becomes

$$Q_L = A_p \dot{x}_p + C_l P_L \tag{2.55}$$

Thus an equivalent equation of load flow Q_L is derived by combining equation (2.55) and (2.53)

$$Q_L = A_p \dot{x}_p + C_l P_L = K_v x_v - K_p P_L \tag{2.56}$$

The actuating piston force F_L is approximately $A_p P_L$, so that piston velocity is relation to spool displacement x_p and load pressure F_L by rearranging equation (2.56)

$$\dot{x}_p = \frac{K_v}{A_p} x_v - \frac{(C_l + K_p)}{A_p} \frac{F_L}{A_p} \tag{2.57}$$

The spool displacement is proportion to input voltage u_v and the valve control input is obtained

$$x_v = k_{iv} u_v \tag{2.58}$$

$$u_v = \frac{x_v}{k_{iv}} = \frac{A_p}{k_{iv} K_v} \dot{x}_p + \frac{(C_l + K_p)}{K_v k_{iv}} \frac{F_L}{A_p} = k_1 \dot{x}_p + k_2 F_L \tag{2.59}$$

where u_v is voltage input of servo valve, k_{iv} is the constant, and k_1, k_2 are simplified constant.

The F_L is desired output force and a control concept of computed force is introduced

$$u_v = k_1 \dot{x}_p^d + k_2 F_L \qquad (2.60)$$

$\dot{x}_p^d$ is modified desired piston velocity

$$\dot{x}_p^d = \dot{x}_{p,d} + K_p \left(x_{p,d} - x_{p,a} \right) \qquad (2.61)$$

, where K_p is a proportion gain. So that the tracking error e is guaranteed to converge to zero when K_p is positive

$$\dot{e} + K_p e = 0, \ e = x_{p,d} - x_{p,a} \qquad (2.62)$$

The control strategy of computed force is shown in Fig. 2.8. Desired load force is added to input voltage command with modified desired piston velocity, and $x_{p,a}$ is feedback of piston length.
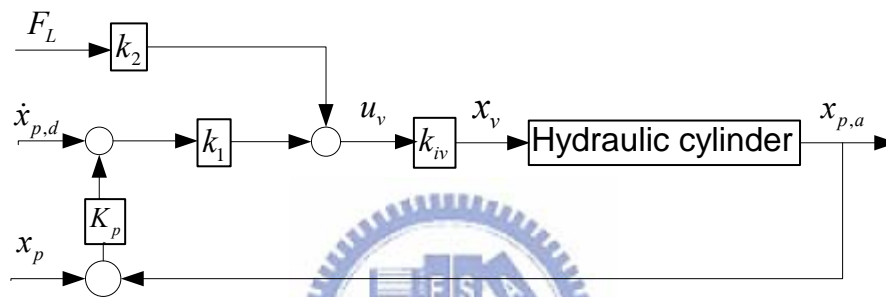
Fig. 2.8 Computed force control strategy

The computed force control strategy can be applied on our hydraulic manipulator. For control of hydraulic manipulator, result of inverse dynamic is adopted for deriving actuating force $\boldsymbol{F_L}$. The computed force of hydraulic manipulator is shown in Fig. 2.9. Link length vector $\boldsymbol{l}$ is identical to piston length, and the subscript d and a are desired and actual condition. Dynamic program is proposed in Sec. 2.3.2., and voltage input $\boldsymbol{u_v}$ of computed force controller is summation of $\boldsymbol{u_1}$ and $\boldsymbol{u_2}$

$$\boldsymbol{u_1} = k_2 \boldsymbol{F_L}, \ \boldsymbol{u_2} = k_1 \dot{\boldsymbol{x}}_p^d \qquad (2.63)$$
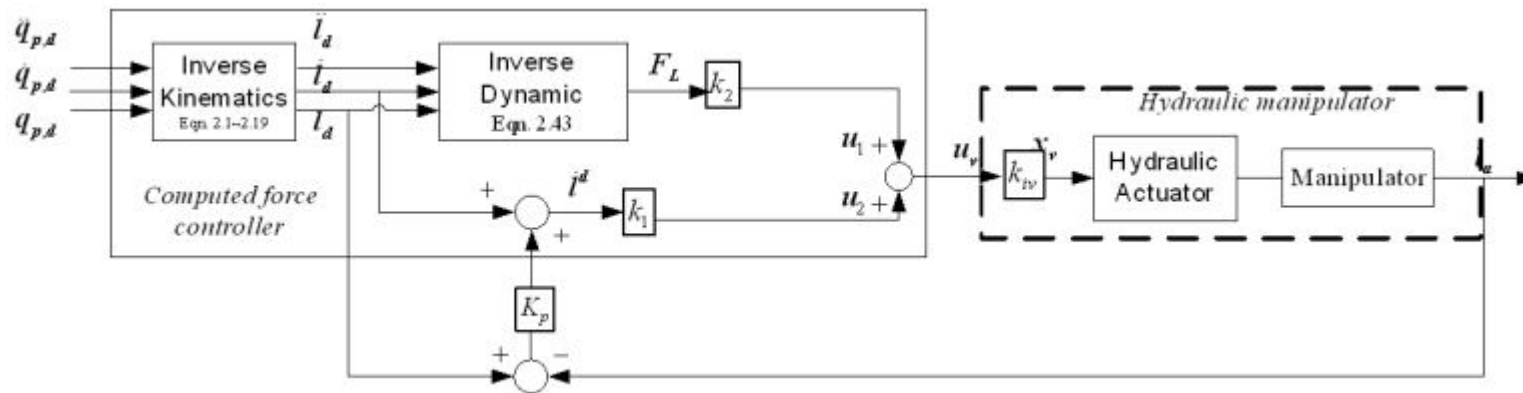
Fig. 2.9. Computed force control for manipulator
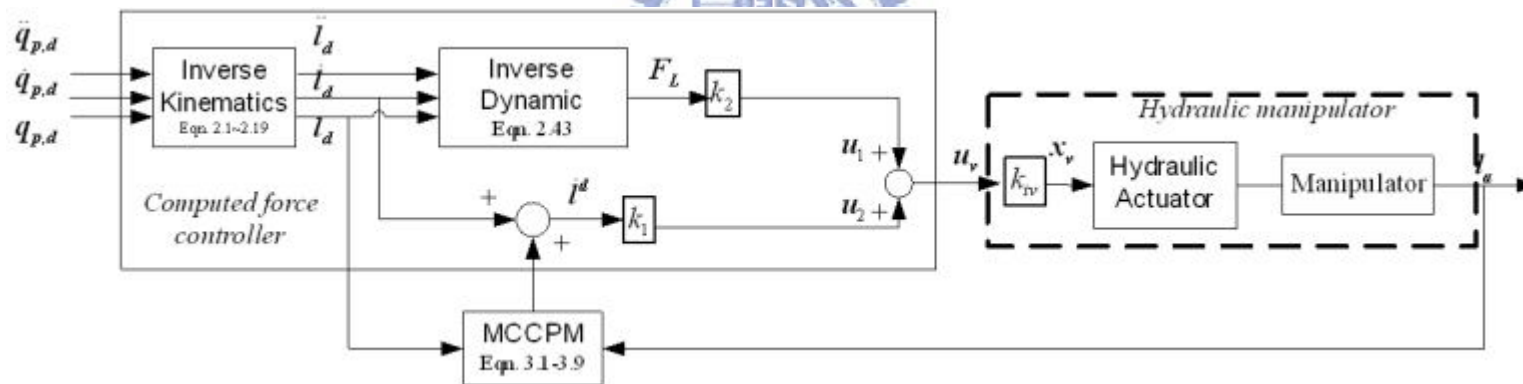
Fig. 2.10. Computed force control with MCCPM for manipulator

Combining with forward dynamic proposed in Sec. 2.5, computer simulator for hydraulic manipulator with dynamics of hydraulic actuators is completely developed, as seen in Fig. 2.11.
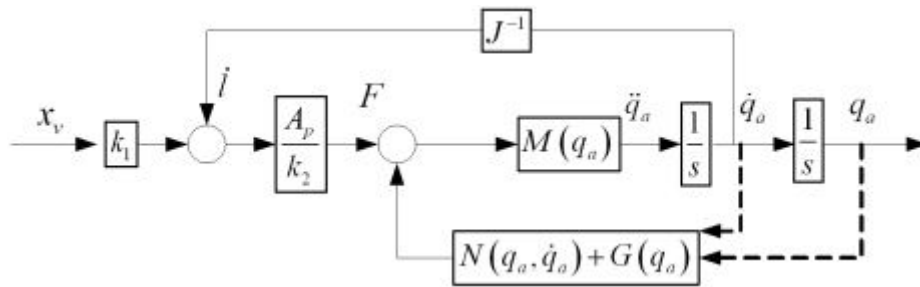
Fig. 2.11. Computer simulator of hydraulic manipulator with hydraulic actuator

2.7 Analysis of workspace

　　Workspace means a territory in which the end-effectors can arbitrarily travel and move. Generally, the workspace of machine tool is as total orientation workspace, TOW. The TOW of parallel manipulator is determined by limits of links' length. Therefore, define TOW of parallel manipulator with mathematical model is defined

$$\Omega_T = \left\{ P \mid Z_{min} \leq z \leq Z_{max}, |X| \leq X_{max}(z) \right\} \text{ , } X \text{ means valuable } \alpha, \beta$$

Pong [25] evaluated the workspace by computing inverse kinematics with discrete value and iteratively examining constraints of link, which is applied in this paper. Analysis program is consisted of several loops to find out the value boundary and the values will be recorded. The flow chart of program and the analysis of workspace are as Fig. 2.12.
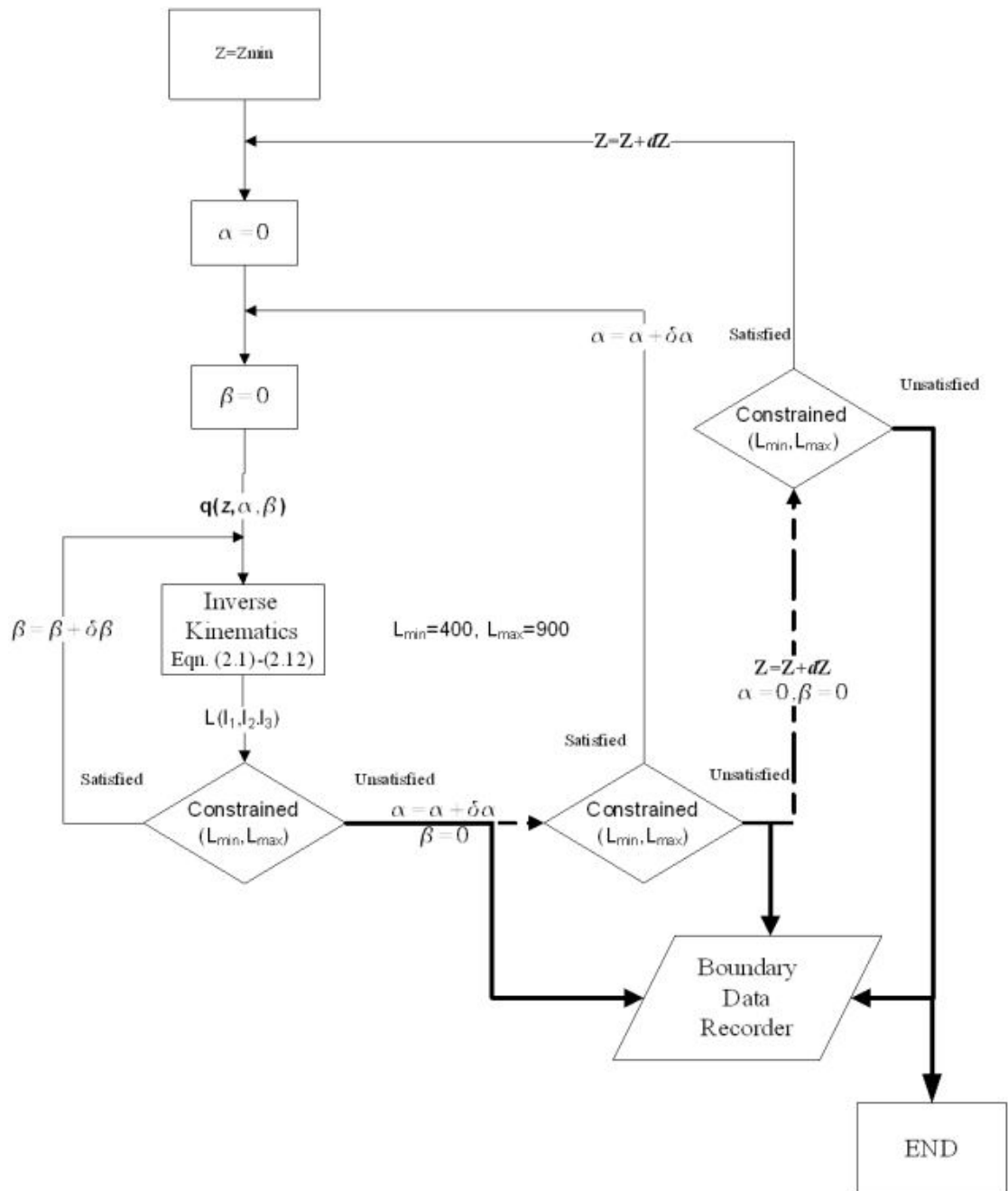
Fig. 2.12. Flow chart of workspace determination programming
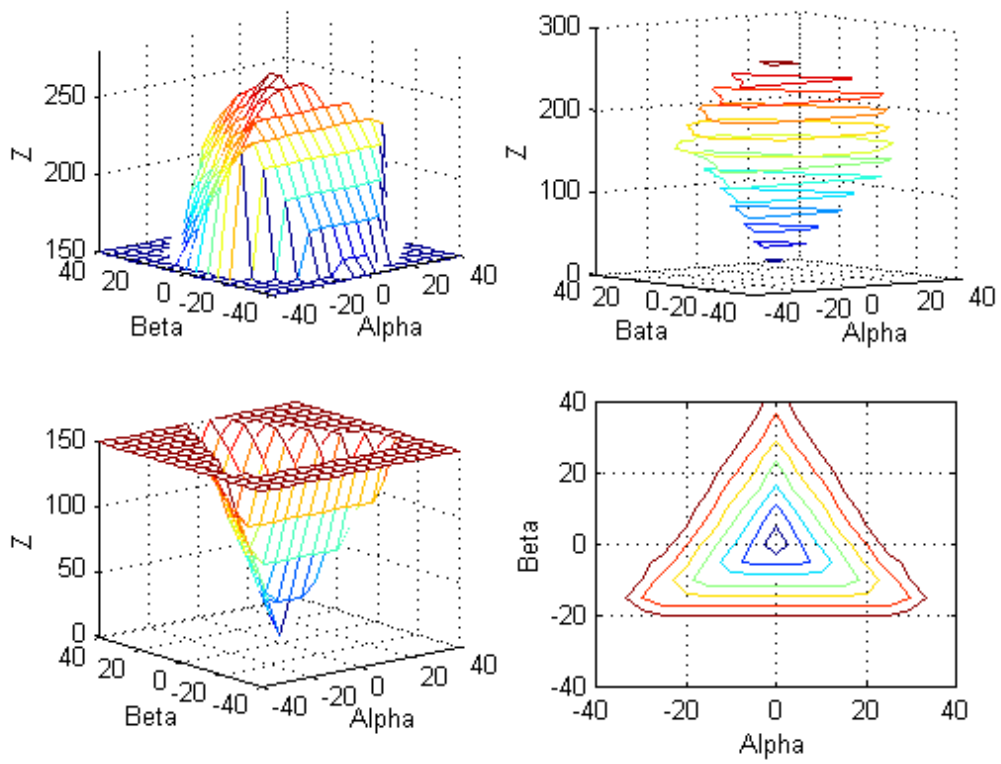
Fig. 2.13. Spatial workspace of Hydraulic Manipulator
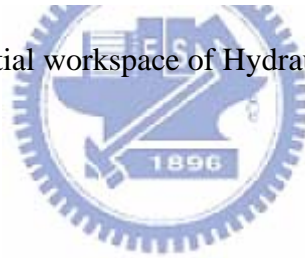
CHAPTER 3
MCCPM AND INTERPOLATION

3.0 Introduction

The MCCPM [10] (Multi-axes Cross-Coupled Pre-compensation) is an algorithm, which was developed by manufacturing laboratory, NCTU. It is for diminishing the trajectory error of manipulators. MCCPM provides a simplified calculation to derive the demand compensative velocity for cutter, if the cutter is not exact on trajectory. In this chapter, MCCPM method is adopted to find out the demand compensative velocity; thereby the error for exact trajectory tracking is compensated previously. In the past, Chin and Lin [29] and Chin and Lu [10] had sequentially governed the MCCPM algorithm; Chin and Tsai [9] has accomplished the feedback gain assignment. And, here, MCCPM is implemented in the system, observing its tracking performance. Behind MCCPM, the interpolation of hydraulic manipulator will be introduced.

3.1 MCCPM controller

MCCPM system includes calculations of contour error and compensative velocity. Trajectory error is defined the deviation in space between desired path and real position; MCCPM compensates trajectory error by calculating needed response velocity and adjusting link velocity to track ideal trajectory. Chin and Lin[29] and Chin and Lu [10] had proposed algorithm of cross-coupled pre-compensation for several years, and the algorithm for compensating of hydraulic manipulator is modified.

3.1.1 Trajectory contour error

The trajectory error is expressed as a 3-dimension vector with L_1, L_2, L_3 elements in joint space. Fig. 3.1 is illustration of path contour error between desired path and actual position.
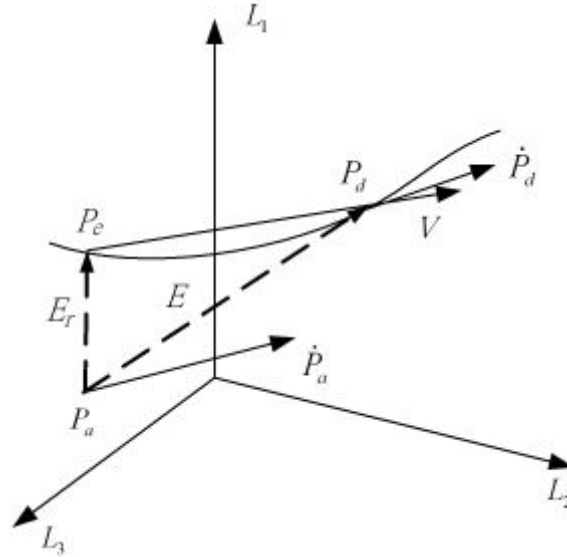
Fig. 3.1. Spatial path contour error

At first, it's assumed that the machining surface is continuous spatial surface. P_a is actual position of pistons, and P_e is the point most close to P_a on the desired path. The vector E is position tracking error vector which is from actual position P_a to desired position P_d.

$$E = P_d - P_a = \begin{bmatrix} E_1 & E_2 & E_3 \end{bmatrix}^T \qquad (3.1)$$

where subscript number means piston's numbering. E_r is the path contour error vector which is the shortest distance between desired trajectory and actual position

$$E_r = P_e - P_a = \begin{bmatrix} E_{r1} & E_{r2} & E_{r3} \end{bmatrix}^T \qquad (3.2)$$

Vector $\vec{V}$ is unit vector expressing the velocity from P_e to P_d. Because the curve is approximately close to straight line, thus the vector $\vec{V}$ can be obtained by taking average of the velocities of P_d and P_a. [10]

$$\overline{V} = \frac{\dot{P}_a + \dot{P}_d}{\left\| \dot{P}_a + \dot{P}_d \right\|} \qquad (3.3)$$

Therefore, the path contour error E_r, is derived as seen in Fig. 3.1

$$E_r = P_e - P_a = E - \overline{P_d P_e} = E - \left(E \cdot \vec{V}\right)\vec{V} = -\left(E \times \vec{V}\right)\times \vec{V} \tag{3.4}$$

Thus E_r is [10]

$$E_r = \begin{bmatrix} E_{r1} \\ E_{r2} \\ E_{r3} \end{bmatrix} = \begin{bmatrix} \overline{V_1}\left(E_3\overline{V_1} - E_1\overline{V_3}\right) + \overline{V_2}\left(E_3\overline{V_2} - E_2\overline{V_3}\right) \\ \overline{V_3}\left(E_1\overline{V_3} - E_3\overline{V_1}\right) + \overline{V_2}\left(E_1\overline{V_2} - E_2\overline{V_1}\right) \\ \overline{V_3}\left(E_2\overline{V_3} - E_3\overline{V_2}\right) + \overline{V_1}\left(E_2\overline{V_1} - E_1\overline{V_2}\right) \end{bmatrix} \tag{3.5}$$

and its distance is

$$dist\left(E_r\right) = \sqrt{1 - \overline{V_2}^2}\,(E_3\overline{V_1} - E_1\overline{V_3}) + \sqrt{1 - \overline{V_1}^2}\,(E_3\overline{V_2} - E_2\overline{V_3})$$
$$+ \sqrt{1 - \overline{V_3}^2}\,(E_1\overline{V_2} - E_2\overline{V_1}) \tag{3.6}$$

From equation (3.5), MCCPM can quickly obtain the actual error E_r. Thus, the compensating velocity can be derived by multiplying a gain value, such as reciprocal of sampling time.

3.2 Pre-compensation velocity

From equation (3.5), the total contour error E_r is obtained

$$E_r = \begin{bmatrix} E_{r1} & E_{r2} & E_{r3} \end{bmatrix}^T \tag{3.7}$$

Error vector E_r is used to calculate the compensative velocity for diminishing contour error. PI controller is applied for modifying velocity. The adjustable velocity can be obtained as

$$\vec{V} = \vec{V}_a + K_v \vec{E}_r + K_{iv} \int \vec{E}_r dt \tag{3.8}$$

and rewritten by vector [7]

$$\vec{V} = \begin{bmatrix} V_1 \\ V_2 \\ V_3 \end{bmatrix} = \begin{bmatrix} V_{a1} + K_v E_{r1} + K_{iv} \int E_{r1} dt \\ V_{a2} + K_v E_{r2} + K_{iv} \int E_{r2} dt \\ V_{a3} + K_v E_{r3} + K_{iv} \int E_{r3} dt \end{bmatrix} \tag{3.9}$$

Hence, the trajectory path can be gradually tracked and the contour error will be diminished.

3.3 Interpolator

The interpolator of hydraulic manipulator is made for trajectory planning, thus the information of machining surface is entered and the interpolator determines fitting trajectory of the tool. For general cutting machine, milling cutter is needed to keep perpendicular to the surface of work piece. In other words, the axis of cutter is normal to machining surface. So the interpolator needs two functions; one is to transform the contour of surface in global space to base frame, and then, from inverse kinematics, the desired lengths of links can be obtained. The other is to instantly calculate the working contour and derive tangential velocity, which will be combined with compensative velocity of MCCPM. In this section, the transformation and interpolation will be introduced and discussed separately.
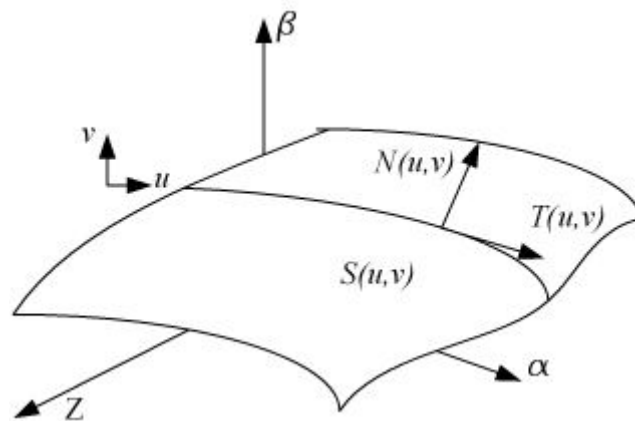
Fig. 3.2. Surface function

3.3.1 Transformation of link trajectory

Like traditional CNC, surface of work piece is designed by smooth fitting curve and bi-cubic spline algorithm is popular fitting patch [30]. Thus, the surface can be expressed as segmental surface functions and with two parameters *u,v*

$$S(u,v) = [S_x \quad S_y \quad S_z]^T (u,v) \tag{3.12}$$

Since it is necessary that the mill cutter is perpendicular to surface, the normal vector of surface *n* must be funded

$$n(u,v) = \frac{\dfrac{\partial S}{\partial v} \times \dfrac{\partial S}{\partial u}}{\left| \dfrac{\partial S}{\partial v} \times \dfrac{\partial S}{\partial u} \right|} \tag{3.13}$$

Because the milling cutter is normal to platform, then the cutter vector based on effectors can be written as

$$Cutter = \begin{bmatrix} 0 & 0 & C \end{bmatrix}^T_{effector} \tag{3.14}$$

where C is length of cutter. Thus, vector *n* should be transformed to cutter vector by Coordinate transformation

$$\begin{bmatrix} 0 \\ 0 \\ C \end{bmatrix}_{effector} = \begin{bmatrix} \cos\beta & 0 & -\sin\beta \\ -\sin\alpha\sin\beta & \cos\alpha & -\sin\alpha\cos\beta \\ \cos\alpha\sin\beta & \sin\alpha & \cos\alpha\cos\beta \end{bmatrix} \begin{bmatrix} n_x(u,v) \\ n_y(u,v) \\ n_z(u,v) \end{bmatrix}_{base} \tag{3.15}$$

and the orientation $\alpha,\ \beta$ are conveniently obtained

$$\alpha = \tan^{-1}\left(\frac{n_y}{\sqrt{n_x^2 + n_z^2}} \right) \ ; \ \beta = \tan^{-1}\left(\frac{n_x}{n_z} \right) \tag{3.16}$$

Therefore, the path and orientation vector of moving platform can be written with parameters as

$$q(u,v) = [x,y,z,\alpha,\beta,\gamma]^T (u,v) = [S(u,v); dir(n(u,v))]^T \tag{3.17}$$

As hydraulic manipulator is responsible for DOF of Z, α, β, then *q* is written

$$q(u,v) = [z \quad \alpha \quad \beta]^T (u,v) = [S_z(u,v) \quad \alpha(u,v) \quad \beta(u,v)]^T \tag{3.18}$$

The vector *q* is inverted to link vector *l* by transforming with inverse kinematics. Thus, the link trajectory can be derived.

3.3.2 Interpolation of 3D surface

Lee [30] had proposed that surface equations, like curve, can be represented as parametric equation. The surface equation is expressed by *bicubic patch method* as a polynomial form

$$S(u,v) = \sum_{i=0}^{3} \sum_{j=0}^{3} a_{ij} u^i v^j \quad (0 \le u \le 1, \ 0 \le v \le 1) \tag{3.19}$$

where parameters u and v are variables ranged 0 to 1.

Rewrite **P**(*u,v*) as a matrix form

$$S(u,v) = \begin{bmatrix} F(u) \end{bmatrix} \begin{bmatrix} S(0,0) & S(0,1) & S_v(0,0) & S_v(0,1) \\ S(1,0) & S(1,1) & S_v(1,0) & S_v(1,1) \\ S_u(0,0) & S_u(0,1) & S_{uv}(0,0) & S_{uv}(0,1) \\ S_u(1,0) & S_u(1,1) & S_{uv}(1,0) & S_{uv}(1,1) \end{bmatrix} \begin{bmatrix} F(v) \end{bmatrix}^T \tag{3.20}$$

where the blending function F is defined [30]

$$\begin{bmatrix} F(u) \end{bmatrix} = \begin{bmatrix} 1 - 3u^2 + 2u^3 & 3u^2 - 2u^3 & u - 2u^2 + u^3 & -u^2 + u^3 \end{bmatrix} \tag{3.21}$$

Tangential vectors respect to **u** and **v** is found

$$\frac{\partial S(u,v)}{\partial u} = \begin{bmatrix} F_u(u) \end{bmatrix} \begin{bmatrix} S & S_v \\ S_u & S_{uv} \end{bmatrix} \begin{bmatrix} F(v) \end{bmatrix}^T$$

$$\frac{\partial S(u,v)}{\partial v} = \begin{bmatrix} F(u) \end{bmatrix} \begin{bmatrix} S & S_v \\ S_u & S_{uv} \end{bmatrix} \begin{bmatrix} F_v(v) \end{bmatrix}^T \tag{3.22}$$

where subscription u,v means differentiation with respect to u,v [30]

$$F_u(u) = \begin{bmatrix} -6u + 6u^2 & 6u - 6u^2 & 1 - 4u + 3u^2 & -2u + 3u^2 \end{bmatrix} \tag{3.23}$$

However, the bicubic patch can only determine the boundary of surface function, and the surface curve is yet unknown.
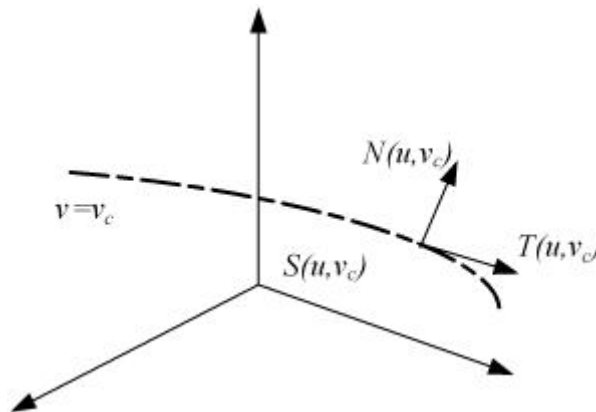
Fig. 3.3. Isoparameter of function S

For deriving the internal shape of surface, isoparametric function is applied, which is fixed one parameter, to determine the curve. The isoparametric curve is defined as Hermite curve

$$S(u, v_c) = \begin{bmatrix} F(u) \end{bmatrix} \begin{bmatrix} S_0(0, v_c) \\ S_1(0, v_c) \\ S_{u0}(0, v_c) \\ S_{u1}(0, v_c) \end{bmatrix} \tag{3.24}$$

where $v=v_c$ is constant variable. As Hermite curve function, the unknown, S_{u0}, $S_{u1,...,}S_{uk,}$ is derived [30]

$$\begin{bmatrix} 3S_1 \text{-} 3S_0 \\ 3S_2 \text{-} 3S_0 \\ \vdots \\ \vdots \\ 3S_k \text{-} 3S_{k\text{-}2} \end{bmatrix} = \begin{bmatrix} 2 & 1 & 0 & \cdots & & \\ 1 & 4 & 1 & \cdots & & \\ & & \cdots & & & \cdots \\ & & 0 & 1 & 4 & 1 \\ & & \cdots & 0 & 1 & 2 \end{bmatrix} \begin{bmatrix} S_{u0}(0, v_c) \\ S_{u1}(0, v_c) \\ \vdots \\ \vdots \\ S_{uk}(0, v_c) \end{bmatrix} \tag{3.25}$$

Hence, from equations (3.23) coefficients of interpolative function is derived, and the total surface, thereby, can be founded by changing fixed parameter v_c.

CHAPTER 4

EXPERIMENT OF HYDRAULIC MANIPULATOR

Computed force control is built on the hydraulic manipulator as described above. Trajectory test is needed for observing the tracking performance of control scheme. Since the platform is operated with computer, the controller is written in program and the results are recorded within files to observe easily. In this chapter, hydraulic manipulator system will be introduced and experimental results of control scheme are exhibited and analyzed.

4.1 Set-up of hydraulic manipulator

Hydraulic manipulator, which was assembled in laboratory, is a simple parallel manipulator with three hydraulic actuators. For avoidance of singular motion, infinite solution in specified positions, the motion platform is constrained by an inclined support, which provides vertical restriction. Three hydraulic cylinders are supplied by oil flow, rate of which is controlled by D1FH (Parker^{TM}) proportional valves. D1FH proportional valve is a 4-position 4-ways valve determined by signal of voltage ranged in ±10 V. Each cylinder connects to platform and basis with two universal joints on both ends, and oil supply is at constant pressure of 10 Bar. Full piston stroke is 400 mm and cylinder length is 500 mm at initial position.

Electronic valve is controlled on PC-Base through two ADDA interface cards of PCI-9111 and ACL-6128. The stroke of piston is measured by potentiometer scale and cards read AD signal from potentiometer to determine the piston length. Since the valve has a band width of 100 Hz of operation, the sampling time of 10 milliseconds. Set-up of hydraulic manipulator with PC-Base is as followed figure 4.1
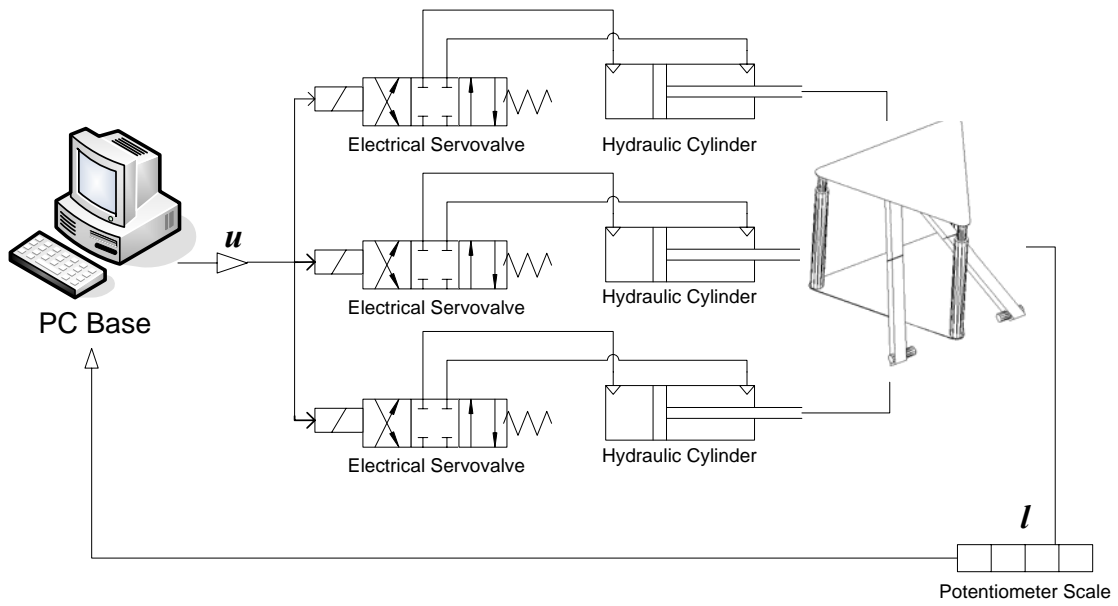
Fig. 4.1. Diagram of hydraulic manipulator control with PC based

4.2 Controller design

Computed force controller is proposed as described above and applied on hydraulic manipulator, as seen in Fig. 4.2.
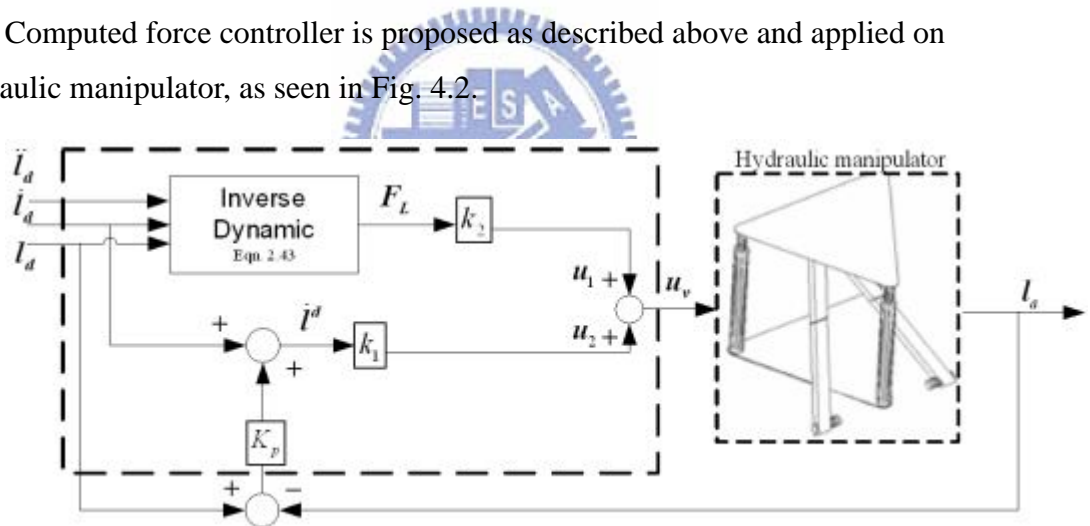
Fig. 4.2. Controller for hydraulic manipulator

Physical constants of hydraulic cylinder are obtained by observing and testing. Relation between spool displacement and cylinder velocity is funded for deriving the constant k_1, and k_2 is obtained by motion test with loading. Relation between spool displacement and velocity is developed by measuring varieties of cylinder velocity with different spool displacement, as seen in Fig. 4.3. Approximate linear relation can be found, and the ratio is reciprocal of constant k_1. Therefore, constant k_1 of each cylinder can be obtained

$$k_1^{cyl1} = 0.0206 \left(\frac{\text{voltage}}{\text{mm/sec}} \right), k_1^{cyl2} = 0.0191 \left(\frac{\text{voltage}}{\text{mm/sec}} \right), k_1^{cyl3} = 0.0202 \left(\frac{\text{voltage}}{\text{mm/sec}} \right)$$

On the other hand, constant k_2 is found by re-developing the relationship with load carry on hydraulic cylinder, as seen in Fig. 4.4. So that, constant k_2 is derived by substituting equation (2.60).

$$k_2 = \frac{u_v - k_1 \dot{x}_p}{F_L} \tag{4.1}$$

and

$$k_2^{cyl1} = 0.0470 \left(\frac{\text{voltage}}{Newton} \right), k_2^{cyl2} = 0.0314 \left(\frac{\text{voltage}}{Newton} \right), k_2^{cyl3} = 0.0314 \left(\frac{\text{voltage}}{Newton} \right)$$

The average force F_L provided by each cylinder is about 100 Newton.
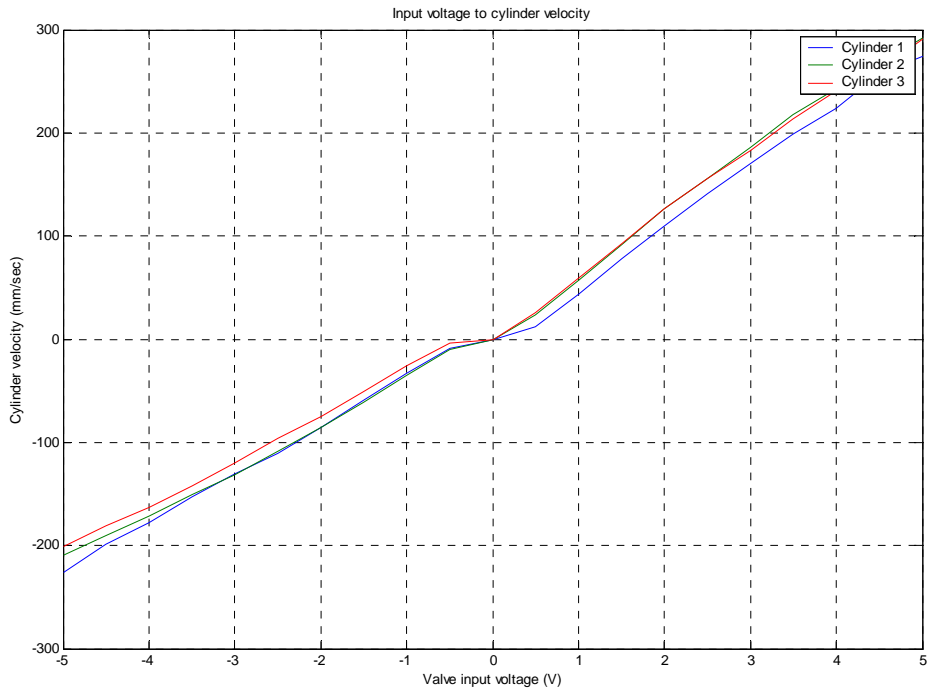
Fig. 4.3. Relation between spool displacement and cylinder velocity
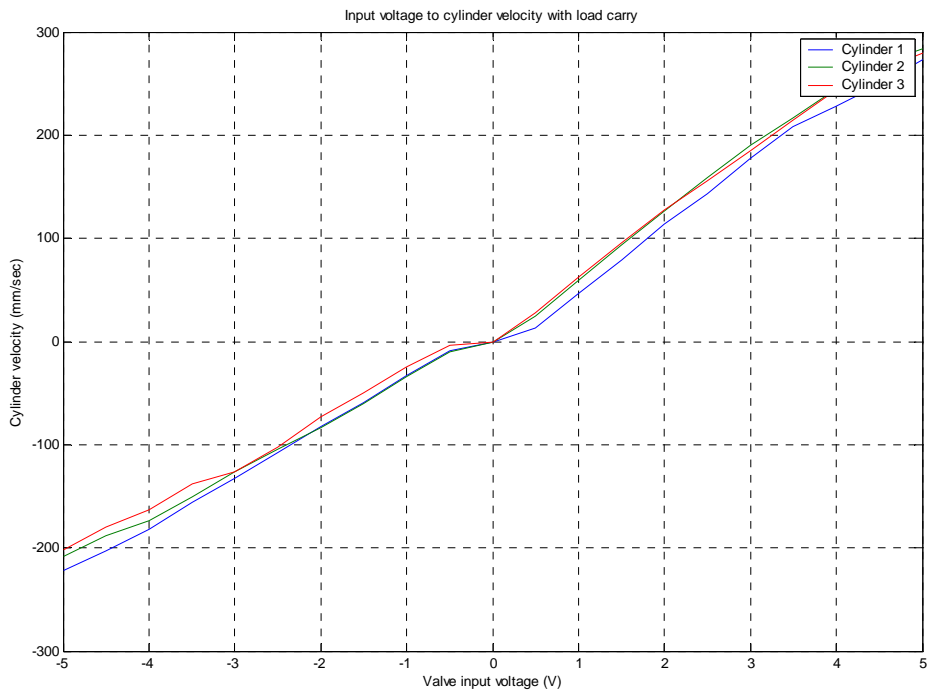
Fig. 4.4. Relation between spool displacement and cylinder velocity with loading

The inverse dynamic program, seen in Fig. 4.2., is utilized to calculate the hydraulic actuating force with PC computing. Therefore, implementation of computer force controller needs detailed information about hydraulic manipulator. The physical parameter of hydraulic manipulator is obtained by approximately estimating with CAD software as seen in Table 4.3. Besides, feedback gain K_p is chosen positive 20 for error convergence as equation (2.62)

$$\dot{e} + K_p e = 0, \ e = l_{p,d} - l_{p,a} \tag{4.2}$$

Table 4.3. Estimated physical parameters

Mass Inertia (kg)		*Moment Inertia* (kg-m^2)	
Piston	6.5	I^{upper}_{axis}	5
Cylinder	7.3	I^{lower}_{axis}	7
Motion platform	8.5	$I^{platform}_{xx}$	0.4538
Dimension of Platform		$I^{platform}_{yy}$	0.7938
$\varphi_a = \varphi_b$	800 mm	$I^{platform}_{zz}$	1.2467
θ	120˚	*Load carry*(kg)	38.5

4.4 Set-up of experiment

For observing performance of control strategy, different trajectories with load are considered, and with additional force computation or not are compared. The complete control scheme is shown in Fig. 4.5 which is implemented system of Fig. 2.9 and 2.10. Experimental trajectory equations are listed on Table 4.4. There are two kinds of experiment, which test, respectively, the performance of computed force controller on cylinder tracking and compare the spatial trajectory with different control strategies. Cylinder trajectory tracking results are shown in Fig. 4.6 and 4.7 series. In Fig. 4.6 series, it compares the performance of cylinder tracking with and without computed force controller, when 38.5kg load carried. Estimated physical parameters are shown in Table 4.3. There are trajectory tracking results of different control strategy are compared in Fig. 4.7. , and the results are exhibited on spatial coordinate with DOF *Z, α, β*, which is derived by forward kinematics from cylinder lengths. These control strategies are respectively: pure velocity controller, velocity with computed force controller, velocity with MCCPM controller, and velocity with computed force and MCCPM controller. These controller structures are shown in Fig. 4.5 individually, and the IAE results of trajectory testing in Fig. 4.6 and 4.7 are shown in Table 4.5. In Fig. 4.5, dynamic function constructed in Sec. 2.3.2 is adopted for computing actuating force,

$$\boldsymbol{F} = Dynamics\left(q,\dot{q},\ddot{q}\right) \tag{4.3}$$

and the MCCPM derives the compensating velocity as equation (3.8).

$$\overline{\boldsymbol{V}} = \overline{\boldsymbol{V}}_a + K_v \overline{\boldsymbol{E}}_r + K_{iv} \int \overline{\boldsymbol{E}}_r dt \tag{4.4}$$

Table 4.4.   Trajectory test in experiments

Trajectory 1	$Z(t) = 650,\ \alpha(t) = \dfrac{\pi}{15}\cos(0.4\pi t),\ \beta(t) = \dfrac{\pi}{15}\sin(0.4\pi t)$
Trajectory 2.	$Z(t) = 650,\ \alpha(t) = \dfrac{\pi}{15}\cos(1.2\pi t),\ \beta(t) = \dfrac{\pi}{15}\sin(1.2\pi t)$
Trajectory 3.	$Z(t) = 600 + 10t,\ \alpha(t) = 0,\ \beta(t) = \dfrac{\pi}{18}\sin(0.4\pi t)$
Trajectory 4	$Z(t) = 650 + 5t,\ \alpha(t) = \dfrac{\pi}{16}\cos(1.2\pi t),\ \beta(t) = \dfrac{\pi}{16}\sin(1.2\pi t)$
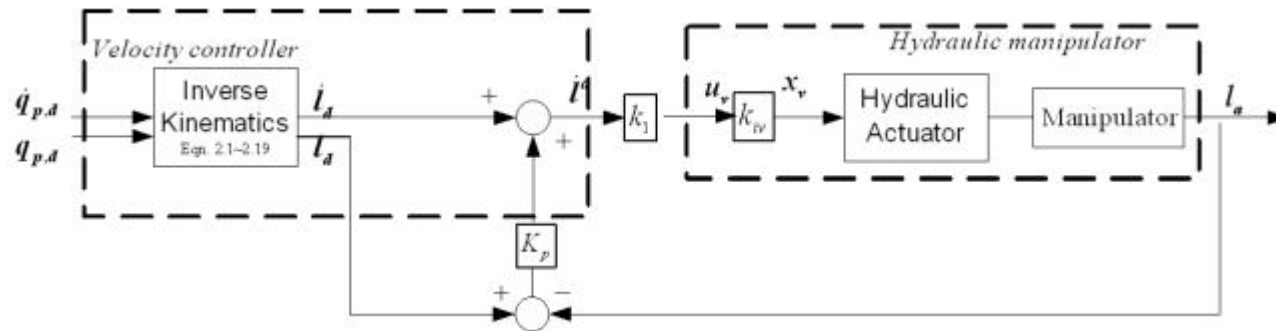
Fig. 4.5. (a) Experiment set-up of hydraulic manipulator (Velocity controller)
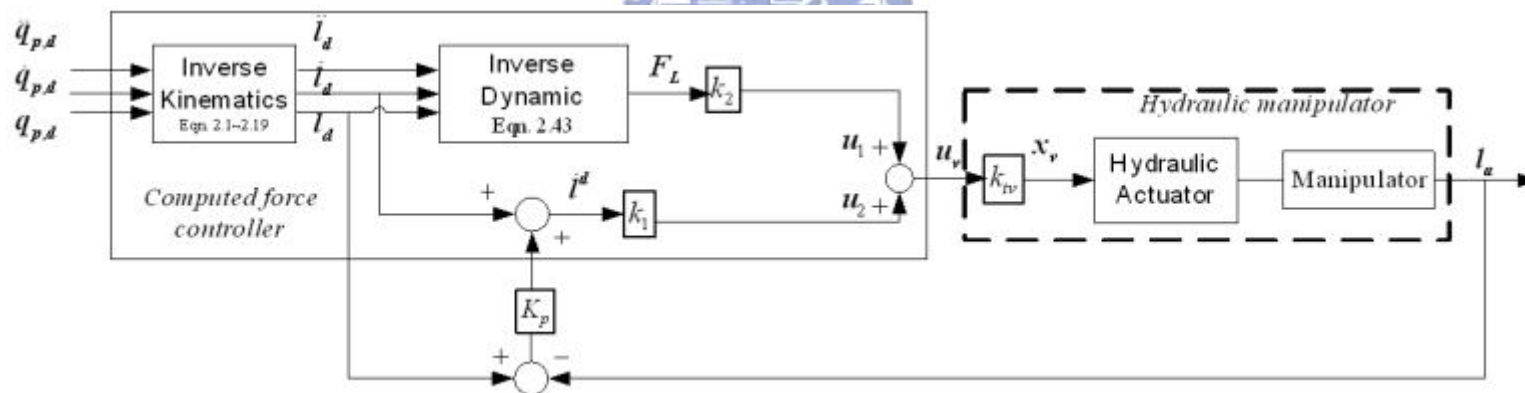
Fig. 4.5. (b) Experiment set-up of hydraulic manipulator (Velocity with computed force controller)
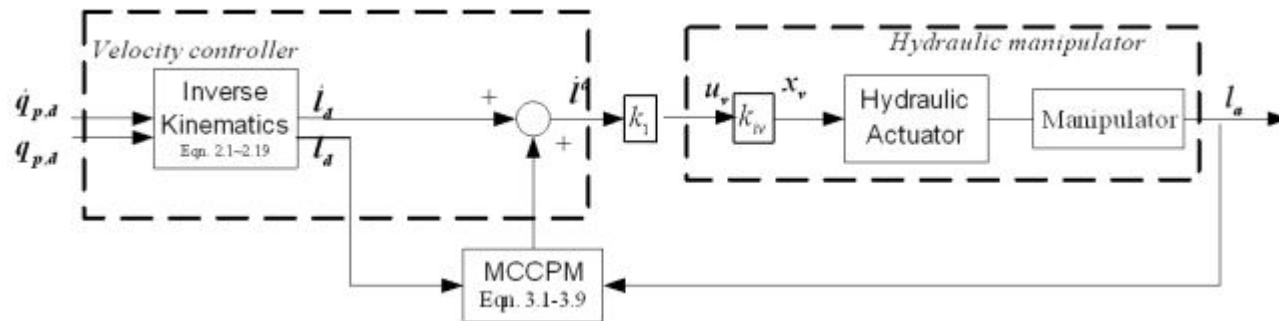
Fig. 4.5. (c) Experiment set-up of hydraulic manipulator (Velocity with MCCPM controller)
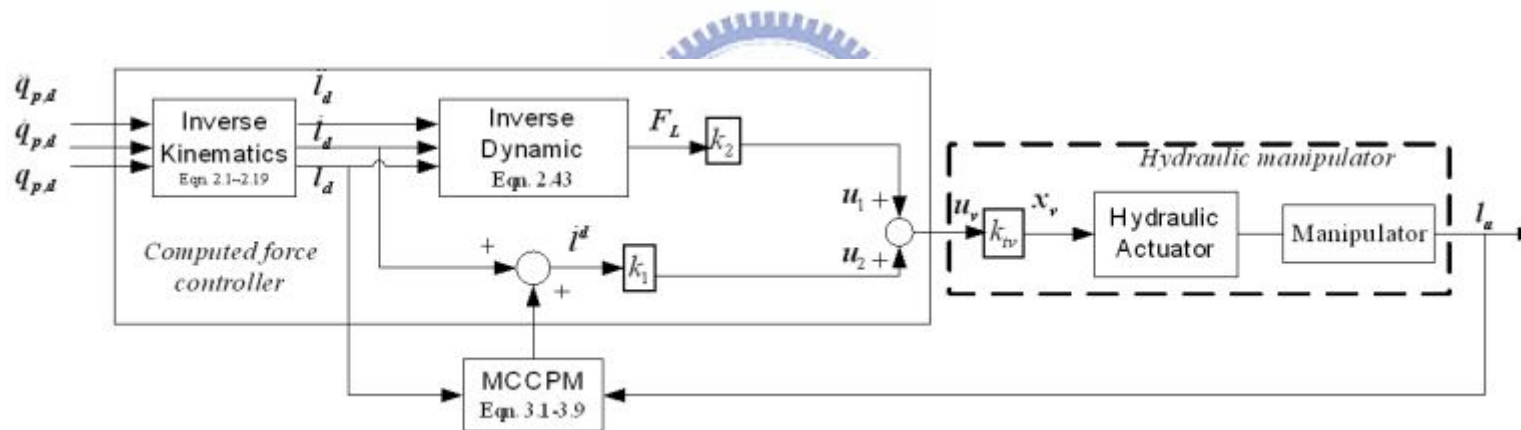
Fig. 4.5. (d) Experiment set-up of hydraulic manipulator (Velocity with computed force and MCCPM controller)

4.5 Experimental result

Comparison of cylinder tracking result on different trajectories with computed force or not is shown in Fig. 4.6 series. *Load carries: 38.5 kg*

Trajectory 1. $Z(t) = 650, \ \alpha(t) = \dfrac{\pi}{15}\cos(0.4\pi t), \ \beta(t) = \dfrac{\pi}{15}\sin(0.4\pi t)$
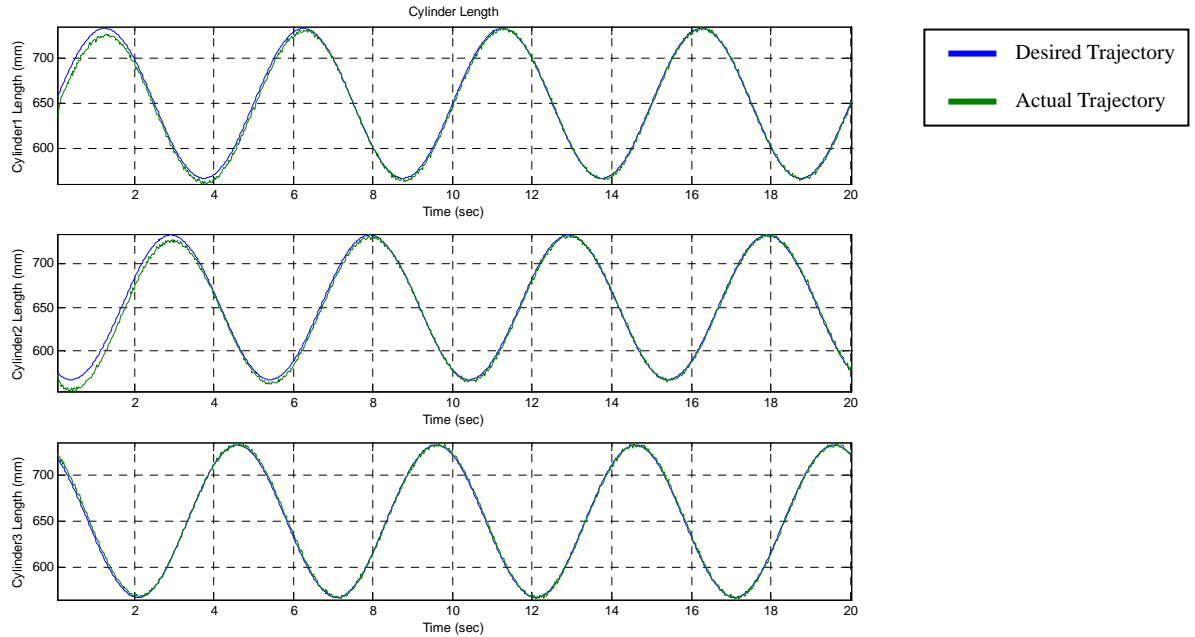
Fig. 4.6. (a) Cylinder tracking **without** computed force (<u>Trajectory 1</u>)
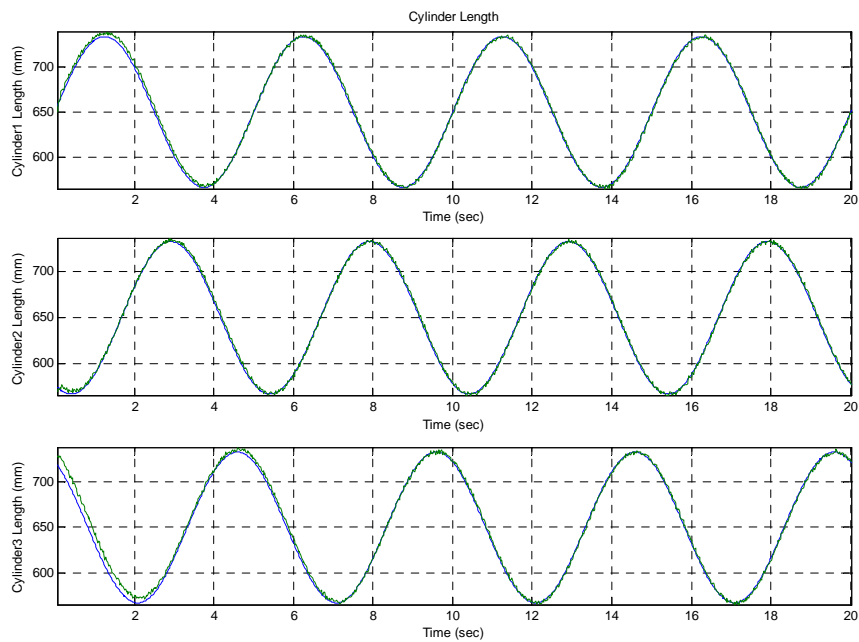
Fig. 4.6. (a) Cylinder tracking **with** computed force (<u>Trajectory 1</u>)

Trajectory 2. $Z(t) = 650,\ \alpha(t) = \dfrac{\pi}{15}\cos(1.2\pi t),\ \beta(t) = \dfrac{\pi}{15}\sin(1.2\pi t)$
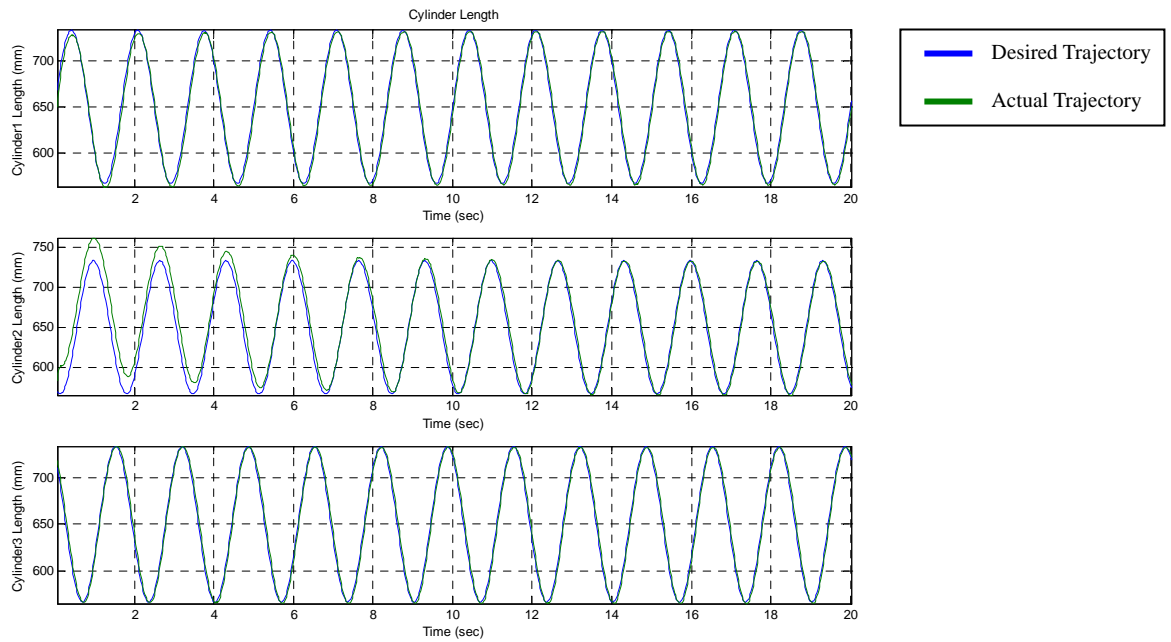
Fig. 4.6. (b) Cylinder tracking **without** computed force (<u>Trajectory 2</u>)
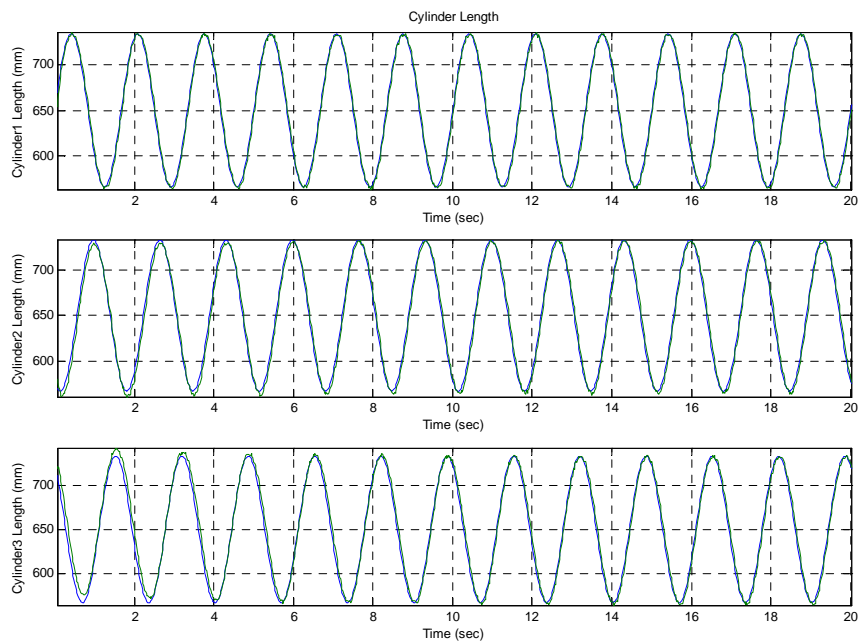
Fig. 4.6. (b) Cylinder tracking **with** computed force (<u>Trajectory 2</u>)

<u>*Trajectory 3.*</u> $Z(t) = 600 + 10t, \ \alpha(t) = 0, \ \beta(t) = \dfrac{\pi}{18}\sin(0.4\pi t)$
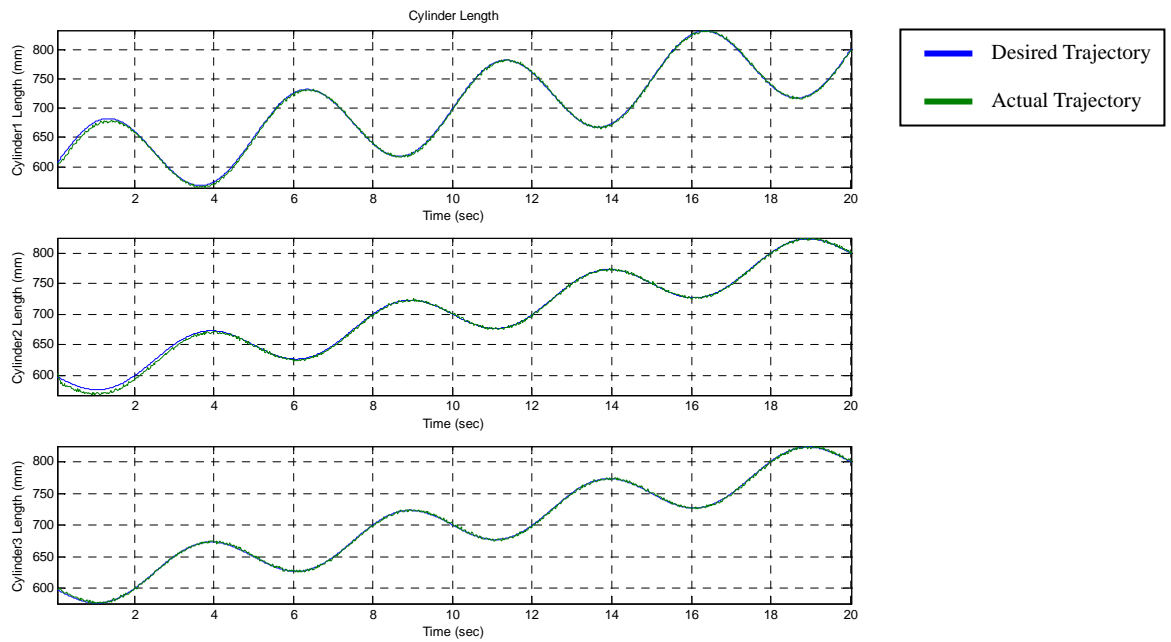
Fig. 4.6. (c) Cylinder tracking **without** computed force (<u>Trajectory 3</u>)

Fig. 4.6. (c) Cylinder tracking **with** computed force (<u>Trajectory 3</u>)

Fig. 4.6. (d) Cylinder tracking **without** computed force (Trajectory 4)

Fig. 4.6. (d) Cylinder tracking **with** computed force (Trajectory 4)

Comparison of control strategies for spatial trajectory tracking is shown in Fig. 4.7 series.
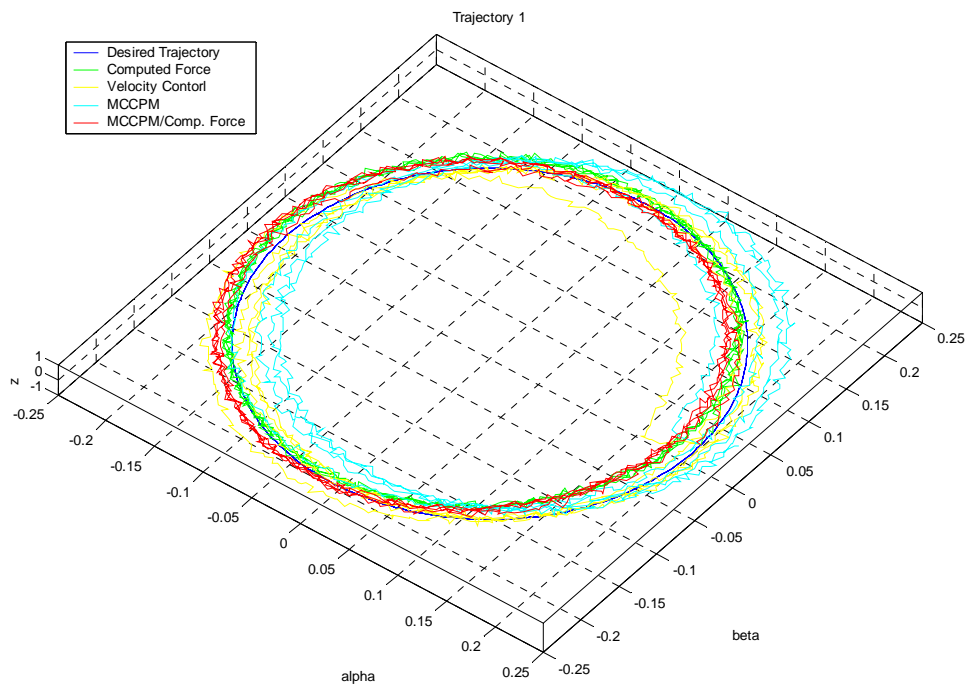
Fig. 4.7. (a) $Z(t) = 650$, $\alpha(t) = \dfrac{\pi}{15}\cos(0.4\pi t)$, $\beta(t) = \dfrac{\pi}{15}\sin(0.4\pi t)$ (Trajectory 1)
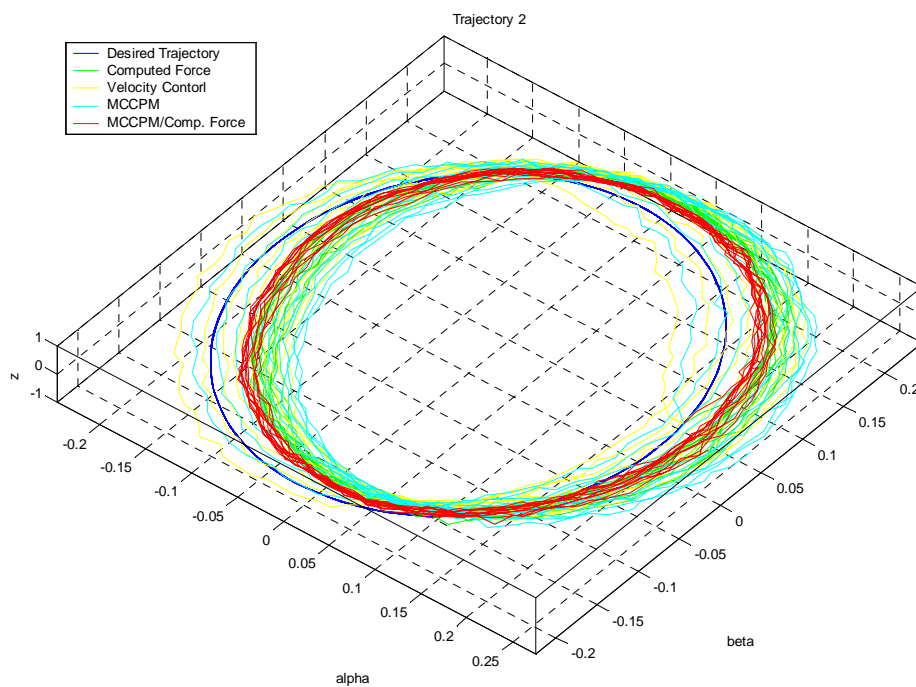
Fig. 4.7. (b) $Z(t) = 650$, $\alpha(t) = \dfrac{\pi}{15}\cos(1.2\pi t)$, $\beta(t) = \dfrac{\pi}{15}\sin(1.2\pi t)$ (Trajectory 2)
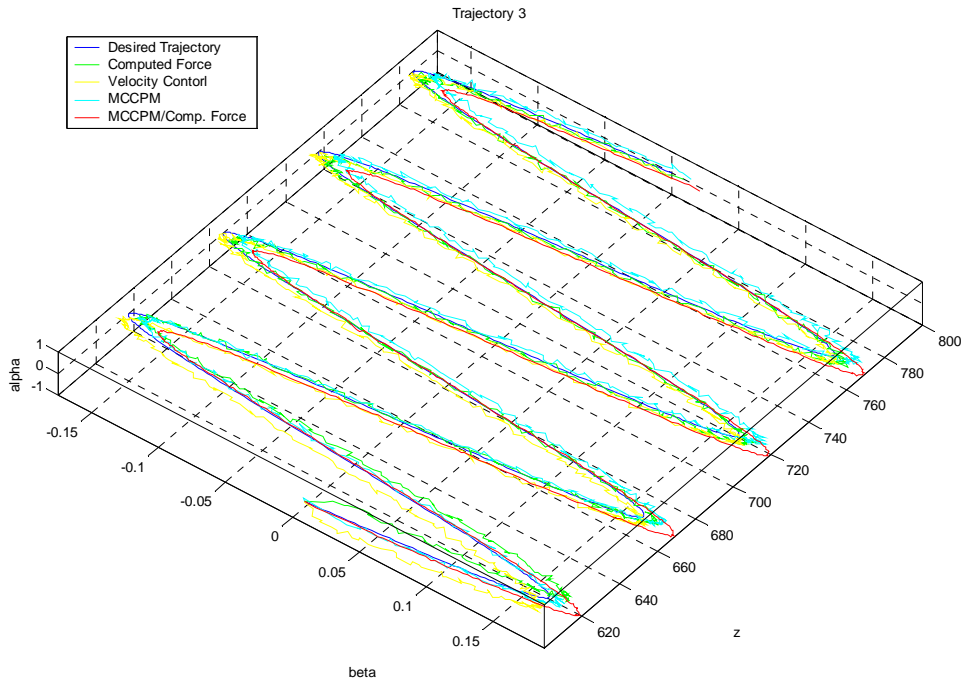
Fig. 4.7. (c) $Z(t) = 600 + 10t,\ \alpha(t) = 0,\ \beta(t) = \dfrac{\pi}{18}\sin(0.4\pi t)$ (Trajectory 3)
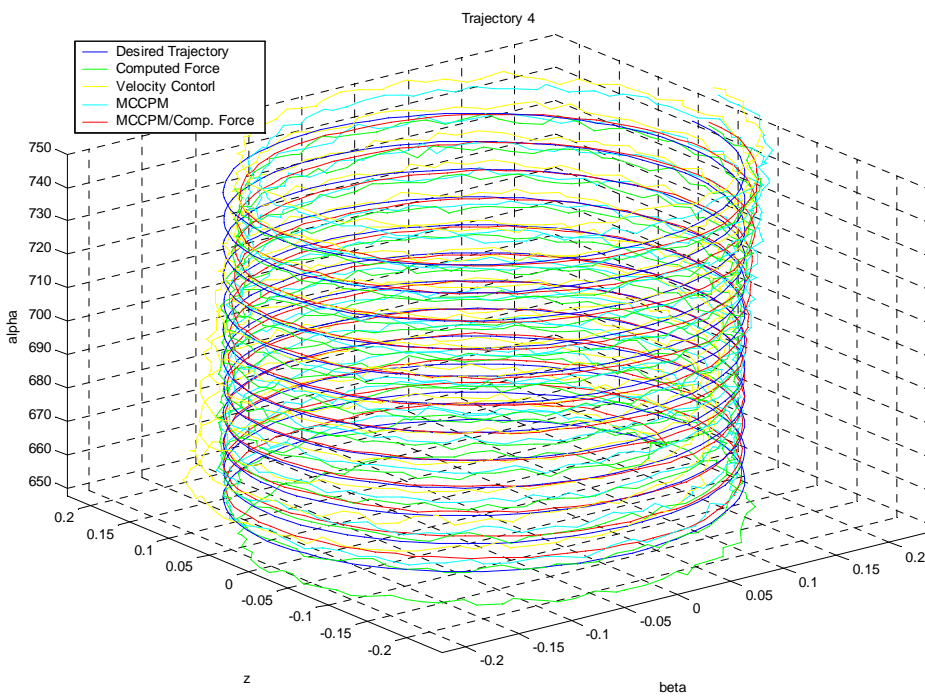
Fig. 4.7. (d) $Z(t) = 650 + 5t,\ \alpha(t) = \dfrac{\pi}{16}\cos(1.2\pi t),\ \beta(t) = \dfrac{\pi}{16}\sin(1.2\pi t)$

(Trajectory 4)

All trajectories is executed on hydraulic manipulator with load carries 38.5 kg. And the observation of tracking results, IAE (integral absolutely error), are shown in Table 4.5. The IAE is given by

$$IAE = \int_t |e(t)|dt = \sum^n |e(t)|T_s \text{ (discrete-time)} \tag{4.5}$$

Table 4.5. (a)   IAE results for trajectory tracking in Fig. 4.6 and 4.7

Experiment 1:

Trajectory Number	Controller type	Cylinder 1	Cylinder 2	Cylinder 3
1	Pure velocity control	61.6361	70.9056	37.7087
	With computed force	42.2071	36.1476	39.8857
2	Pure velocity control	90.6020	178.7620	87.6744
	With computed force	74.9317	97.9322	84.5020
3	Pure velocity control	41.0597	46.7235	47.2582
	With computed force	39.8707	43.7352	24.9348
4	Pure velocity control	162.8768	202.9674	88.6916
	With computed force	97.3378	176.5577	83.3361

Table 4.5. (b)   IAE results for trajectory tracking in Fig. 4.6 and 4.7

Experiment 2:

Trajectory Number	Controller type	Cylinder 1	Cylinder 2	Cylinder 3
1	Velocity with MCCPM	71.9277	144.0352	64.3222
	Velocity with computed force　and MCCPM	33.8746	33.7042	41.3258
2	Velocity with MCCPM	82.0107	182.5960	88.5417
	Velocity with computed force　and MCCPM	75.8850	74.4454	78.5547
3	Velocity with MCCPM	43.2597	34.4584	24.5886
	Velocity with computed force　and MCCPM	28.2688	36.7982	45.8500
4	Velocity with MCCPM	183.4489	181.3060	91.3014
	Velocity with computed force　and MCCPM	74.4102	89.7602	81.6863

4.6 Result analysis and discussion

As seen in Table 4.5 (a), trajectory tracking ability is good when its IAE is small. In experiment 1, the total IAE is smaller when computed force control is applied than not applied. The IAE shows that the computed force control has improved tracking result. By applying computed force controller, the converging rate of error is increasing, as seen in Fig. 4.6 series, so that the IAE is reduced. Therefore, the computed force controller has apparent contribution on trajectory tracking with load carried. Fig. 4.6. (c) and (d) show that the tracking ability of pure velocity control is poor at high frequency motion, but, however, the implemented computed force controller can provide compensative command to help track rapidly. Whereas, in slower motion, loading has slight effect on manipulator, therefore, performance of computed force has less contribution on tracking, as proven in Fig. 4.6. (a) and (c).

In experiment 2, different control strategy is applied on manipulator and the trajectory tracking results are shown in Fig. 4.7 series. From IAE result in Table 4.5 (b), the MCCPM controller can also improve the tracking by compensating trajectory error. Therefore, the combination of computed force combined MCCPM controller can theoretical improve the trajectory accuracy as high load carry, and it's proven by IAE results in Table 4.5 (b).
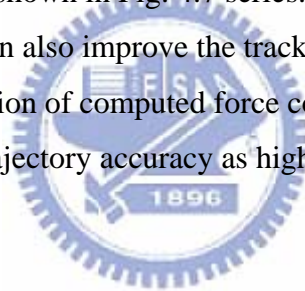
CHAPTER 5
CONCLUSION

The computed force controller for hydraulic manipulator has been proposed and implemented. As experiment, the attempt is successful and results are satisfactory. With computed force control, the trajectory tracking of hydraulic manipulator is improved, and the trajectory error is reduced. On the other hand, combination of computed force and MCCPM, spatial trajectory has better performance as estimated. For construction of accuracy computed force, the dynamic parameter should be clear and definite to compute approximate force. In addition, physical constants of hydraulic actuators need to be calibrated precisely. As experimental results, for light load or slow motion, the computed force controller has less contribution, and even impracticable. However, for high loading or velocity motion, it's necessary to implement computed force control to improve the control ability of hydraulic actuator, especially for advanced machine tool.Although we implement it in our manipulator for trajectory accuracy, it is suitable for being applied to any application.

CHAPTER 6

<u>**FUTURE WORK:**</u>

EXTERNAL FORCE MODEL AND CONCEPT OF ADAPTIVE
CONTROLLER

6.0 Introduction

Generally speaking, machine tool may all encounter external effects making it deterioration performance. These external effects, like friction and cutting force, do vary with several distinct environmental factors, for instance, material characteristics of work piece or machining force. Because of high nonlinearity and dynamical uncertainty, these external effects indeed cannot be modeled. Additionally, dynamic of the hydraulic machine is also perplexedly modeled, for its complex coupled system and nonlinearity. Hence, for accurately control as currently ordinary technologies, it's necessary to apply advanced control strategy for adapting model dynamic by feedback compensating.

In common control technology, model-based adaptive control is successful to use on systems with dynamical parametric uncertainty. As results [14] [31], adaptive control has high efficiency in robot manipulator and trajectory tracking with PD controller. Honegger [11] implemented adaptive control for Hexaglide parallel milling machine, similar to Stewart platform, and he proposed simplification of dynamics of machine for easily parameters updating. Otherwise, many new approaches for simplifying external force, as friction, were proposed. Alonge *et al* [32] identified friction as a dynamics model and degraded it with adaptive control. Likewise, Panteley *at el* [33] treated friction as a disturbance and parameterized it for adaptive updating.

An adaptive control is investigated for advanced control of manipulator. First, the external force model is defined, including the friction force model [1] and cutting force model [7]. Second, we consider the dynamics of manipulator and develop its parameterization, including external effects. Further, Lyapunov candidate function is chosen, and the convergence condition can be defined for achieving adaptive law and guarantee the stability of system.

This chapter provides a control concept for future development and implementation on such parallel cutting machine. However, it's not implemented on

our hydraulic manipulator.

6.1 Models of external force

Friction plays a significant role on mechanism dynamic and cannot be neglected in actual machine, but it is difficult to predict and compute for its highly nonlinear and uncertain characteristics. In system, parameters estimation is applied for computing friction effect and increasing the stability of machine. In past research, friction force was modeled in several papers; Canudas *et al* [1] developed a friction model that contains several nonlinear terms with assumption of bristle contact. Eleonor *et al* [33] investigated the effect of friction on prismatic joint and built frictional dynamics with Lagrange differential equations. Elena *et al* treated friction as a disturbance and parameterized it with adaptive controller. In this section, friction model [1] is adapted to adjust our inherent dynamical model.

On the other hand, cutting force can be also treated as external disturbance as friction. For different of material, feed rate, and revolution of axis, cutting force reacted on tool cutter varies. Besides uncertainties, cutting force is complex and nonlinear. As the results, it affects the stability of machine and is difficult to control. Tlusty [34] had developed model of cutting force in end milling into elements, and Li *et al* [2] derived cutting force in three dimensions. As their modeling of cutting force, the reaction of cutting force can be simplified. In this case, model of cutting force is adopted to simulate real condition and discuss its stability.

6.1.1 Frictional force

As Canudas *et al* [1] research, touch of two rigid bodies is seen as contact through elastic bristles. As relative velocity *v* is made, the bristle will deform as stiff spring. Then, the friction force is caused by bristle deflection as

$$F = \sigma_0 z + \sigma_1 \frac{dz}{dt} + \sigma_2 v \tag{6.1}$$

where *z* is average deflection of bristles, σ_0 the stiffness, σ_1 the damping coefficient, and σ_2 can be treated as Coulomb coefficient.
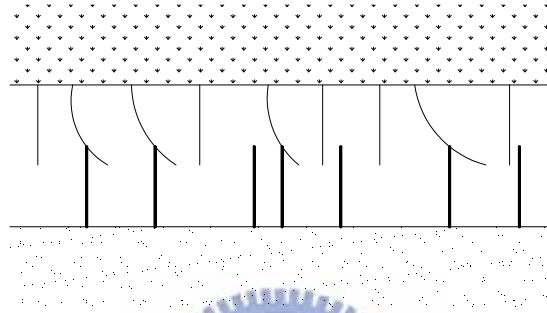
Fig. 6.1. Elastic bristle model

The differential of deflection is correlated to *v* as

$$\frac{dz}{dt} = v - \frac{|v|}{g(v)} z \tag{6.2}$$

where *g(v)* is corresponding function which is monotonically decreasing with *v*. And function *g* is derived

$$\sigma_0 g(v) = F_{co} + (F_s - F_{co}) e^{-(v/v_s)^2} \tag{6.3}$$

where F_{co} is Coulomb friction force, F_s is Stribeck force, and v_s is Stribeck velocity. From Equations (6.1)-(6.3), a friction force function *F(v)* is developed with variable *v* and its direction is opposite to that of body movement.

$$F_f = -F(v)\mathrm{sgn}(v) \tag{6.4}$$

The friction model is applied on prismatic, and universal joints of the hydraulic links. The friction force on links can be rewritten as $F_f = -F(\dot{l})\mathrm{sgn}(\dot{l})$. Since the friction force is uncertain model, the coefficients and constants is assigned, σ_0, σ_1, σ_2, *etc,.* , adaptive parameters and adopt those by feedback estimation.

6.2 Cutting force

Before modeling cutting force, the coordinate system should be defined initially. As figure, x,y is Cartesian coordinate system fixed on cutter with its origin locating on interaction between cutter axis and work face.
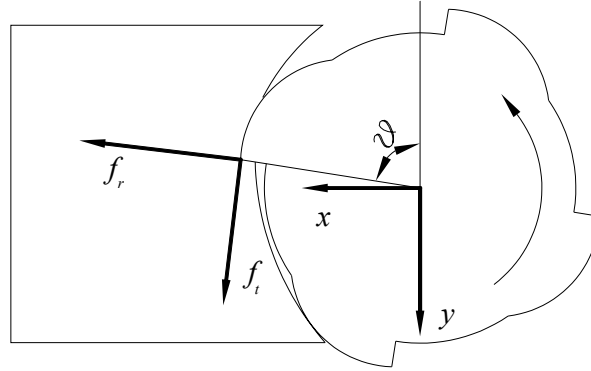
Fig. 6.2. Milling cutter

From Li *et al* [2], the tangential cutting force is a function obtained from the chip thickness and other empirical constant.

$$\tilde{f}_t = K_t t_c \cdot dz = K_t t_x \sin \phi(t) \cdot dz \qquad (6.5)$$

t_c is the chip thickness, and $\tilde{f}_t$ is elemental force of discrete parts with interval dz of cutter, $\varphi(t)$ varies with height

$$\phi(t) = \omega \cdot t + \theta_c \cdot z \qquad (6.6)$$

Thus, the radial and axial force can be obtained as

$$\tilde{f}_r = K_r \tilde{f}_t \,, \tilde{f}_a = K_a \tilde{f} \qquad (6.7)$$

where K_t , K_r , K_a are tool parameters.

Transfer these polar forces to forces in Cartesian system with transformation matrix

$$\begin{bmatrix} \tilde{f}_x \\ \tilde{f}_y \\ \tilde{f}_z \end{bmatrix} = \begin{bmatrix} \cos\theta & \sin\theta & 0 \\ \sin\theta & -\cos\theta & 0 \\ 0 & 0 & 1 \end{bmatrix} \begin{bmatrix} \tilde{f}_t \\ \tilde{f}_r \\ \tilde{f}_a \end{bmatrix} \qquad (6.8)$$

Since above forces are partial, the total forces reacting on cutter are summation of elemental forces

$$\begin{bmatrix} F_{c,x} \\ F_{c,y} \\ F_{c,z} \end{bmatrix} = \sum \begin{bmatrix} \tilde{f}_x \\ \tilde{f}_y \\ \tilde{f}_z \end{bmatrix} \qquad\qquad (6.9)$$

Cutting force highly depends on by case, and as difficult precise computed as friction. Generally, it is treated as a kind of disturbance [35] and controlled with conventional PID controller. Recently, optimal cutting/milling methods or adaptive feeding modification [36] are proposed for machining efficiency. Nevertheless, modeling cutting force is hard to achieve and with numerous, complicated, and time-wasted computation. In our system, cutting force is added in feedback loop and even computed with adaptive controller. The external force model can also be used in our control system for more accurate force compensation, and the controller could be modified as Fig. 6.3.
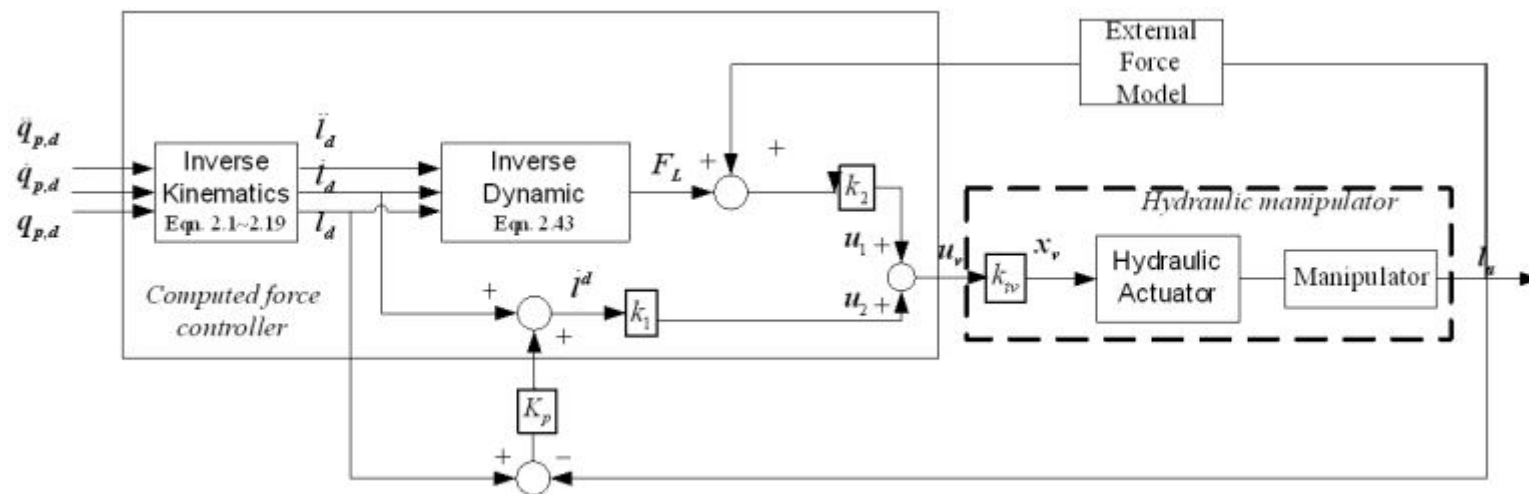
Fig. 6.3. Control system with external force consideration modified from Fig. 2.9

6.3 Parameterized model

The dynamic of machine tool stated above is considered, and derive the dynamic equation [23]

$$F = M(q)\ddot{q} + N(q,\dot{q}) + G(q) \qquad (6.10)$$

where F is the force/torque vector of end-effector in Cartesian space

$$F = \begin{pmatrix} f_z & \tau_\alpha & \tau_\beta \end{pmatrix}^T \qquad (6.11)$$

, q is coordinate vector, M is inertia matrix of machine, N is Coriolis and centrifugal force/torque, and G is gravity force/torque.

The forces of limbs F are derived from multiplying τ by Jacobian matrix J [23]

$$F = {}^B J^T \tau \quad , \quad F = \begin{pmatrix} f_1 & f_2 & f_3 \end{pmatrix}^T \qquad (6.12)$$

Since links enforce, dynamics of the links should be calculated rather than platform from Equation 6.11 as

$$F = M_l(q_a)\ddot{l} + N_l(q_a,\dot{q}_a) + G_l(q_a) \qquad (6.13)$$

where the subscript a means actual coordinate vector.

For adaptive control, the dynamics is described as a simplification form by parameterization

$$F = M_l(q_a)\ddot{l} + N_l(q_a,\dot{q}_a) + G_l(q_a) = Y(q_a,\dot{q}_a,q_d,\dot{q}_d,\ddot{q}_d)\theta \qquad (6.14)$$

Citing dynamical equations in Chapter 2, link forces can be obtained by inverse dynamics, which is quoted as

$$f_i = m_u(a_{iu} - G) \cdot {}^B n_i - f_i^a \qquad (6.15)$$

, but, however, the dynamic forms are highly coupled and complex. It is difficult and inconvenient that the dynamic equation is dissembled to parametric forms. In above equation, term f_i^a, is reacted force from moving platform along to joint axis, and it is obtained through multiplying platform inertia by Jacobian matrix. So, for simplification of computation, some parametric substitutions are made for coupled terms in original equation. Component force f_i^n normal to joint axis and reaction moment M_i are expressed as parameter rather than coupled form. As such simplification, the linearity is developed regressor matrix Y [11]

$$Y\left(q_a, \dot{q}_a, q_d, \dot{q}_d, \ddot{q}_d\right)$$

$$= \left[\left(a_{iu} - G\right) \cdot {}^B n_i \quad -J^T\begin{pmatrix}\left(G - \ddot{x}_P\right)_z \\ 0_{2\times 1}\end{pmatrix} \quad -J^T\begin{pmatrix} 0 \\ \left(-\alpha_P + \omega_P \times \omega_P\right)_{x,y}\end{pmatrix} \quad -J^T\begin{pmatrix} 1 \\ 0_{2\times 1}\end{pmatrix} \quad -J^T\begin{pmatrix} 0 \\ 1_{2\times 1}\end{pmatrix}\right]$$

(6.16)

and parameter vector

$$\theta = \begin{bmatrix} m_u & m_P & I_P & F_n & M_n \end{bmatrix}^T$$ (6.17)

The values in regressor matrix Y are derived from function of variables, which are measured and desired values, and parameter vector ϑ contains simplicity of acted force/moment. Actually, external forces, including friction and cutting force, must be considered. With friction, the actuating force should be rewritten as

$$F = M_l\left(q_a\right)\ddot{l} + N_l\left(q_a, \dot{q}_a\right) + G_l\left(q_a\right) + F_f\left(\dot{l}_a\right)$$ (6.24)

, where F_f is friction forces, which are reacted on limbs, respect to limb velocity. In this case, all frictions reacting on limbs are considered about, including those on prismatic/universal joints, or on actuators. To derive friction problem, the friction model (6.1)-(6.3) is rearranged [33]

$$F_{f,j}\left(\dot{l}_j\right) = \left(\sigma_{0j} - \sigma_{1j}\sigma_{0j}a_j\left(\dot{l}_j\right)\right)z_j + \left(\sigma_{1j} + \sigma_{2j}\right)\dot{l}_j \quad , j=1,2,3$$ (6.25)

where

$$a_j\left(\dot{l}_j\right) = \frac{\left|\dot{l}_j\right|}{F_C + (F_S - F_C)e^{-\left(\dot{l}/l_c\right)^2}}$$ (6.26)

In [33] research, the friction force can be separated into two functions relatively, and, similarly, the frictional dynamics are adopted in parametric form as

$$F_f\left(\dot{l}\right) = F_d\left(\dot{l}, z\right) + Y_f\left(\dot{l}\right)\theta_f$$ (6.27)

where

$$Y_f\left(\dot{l}\right) \triangleq diag\left(\dot{l}_j\right) \quad \text{and} \quad \theta_f \triangleq \begin{bmatrix}\sigma_{1j} + \sigma_{2j}\end{bmatrix}^T$$ (6.28)

The deflection z is not measurable, but, however, in physical aspect, it can be assumed to be restricted so that the first term of the force can be bounded as

$$\left|F_d\left(\dot{l}, z\right)\right| = \left|\left(\sigma_{0j} - \sigma_{1j}\sigma_{0j}a_j\left(\dot{l}_j\right)\right)z_j\right| \le \varepsilon_j + \frac{\varepsilon_j}{\alpha_{1j}}\left|\dot{l}_j\right|$$ (6.29)

As the result, the inequality is utilized to be convergent limit, parameterize the bounded function as

$$F_d\left(\dot{i}, z\right) = Y_d\left(\dot{i}\right)\theta_d \tag{6.30}$$

where

$$Y_d\left(\dot{i}\right) \triangleq \left[diag\left(1_j\right), diag\left(\left|\dot{i}_j\right|\right) \right] \quad \text{and} \quad \theta_d \triangleq \left[\varepsilon_j \cdots, \frac{\varepsilon_j}{\alpha_{1j}} \cdots \right]^T \tag{6.31}$$

Then the friction model is parameterized as

$$F_f\left(\dot{i}\right) = Y_d\left(\dot{i}\right)\theta_d + Y_f\left(\dot{i}\right)\theta_f \tag{6.32}$$

Subsequently, a complete dynamic model in parametric form with consideration of friction forces is developed

$$\begin{aligned}
F &= \begin{bmatrix} f_1 & f_2 & f_3 \end{bmatrix}^T \\
&= M_l\left(q_a\right)\ddot{l} + N_l\left(q_a, \dot{q}_a\right) + G_l\left(q_a\right) + F_f\left(\dot{i}_a\right) \\
&= Y\left(q_a, \dot{q}_a, q_d, \dot{q}_d, \ddot{q}_d\right)\theta + Y_d\left(\dot{i}_a\right)\theta_d + Y_f\left(\dot{i}_a\right)\theta_f
\end{aligned}$$

$$\tag{6.33}$$

Rewrite the parametric model in compact form with separated dynamic and friction force

$$\begin{aligned}
F &= \begin{bmatrix} f_1 & f_2 & f_3 \end{bmatrix}^T \\
&= Y\left(q_a, \dot{q}_a, q_d, \dot{q}_d, \ddot{q}_d\right)\theta + Y_f\left(\dot{i}_a\right)\theta_f
\end{aligned} \tag{6.34}$$

where compact friction model is combined as

$$Y_f\left(\dot{i}\right) = \left[diag\left(\dot{i}_j\right), diag\left(1_j\right), diag\left(\left|\dot{i}_j\right|\right) \right] \tag{6.37}$$

and

$$\theta_f = \left[\left(\sigma_{1i} + \sigma_{2i}\right) \quad \varepsilon_i \quad \frac{\varepsilon_i}{\alpha_{1i}} \right], \quad i = 1, 2, 3 \tag{6.38}$$

6.4 Stability and adaptation algorithm

For adaptive control strategy, the stability of system, which contains minimal joint error and variation of parameter values, must be confirmed. Craig [3], proposed Lyapunov function candidate to ensure the stabilization of error of joints and parameters, and then develop adaptive law. For funding Lyapunov function, the

dynamics function should be requested

$$F = Y(q_a, \dot{q}_a, q_d, \dot{q}_d, \ddot{q}_d)\theta + Y_f(l)\theta_f \qquad (6.39)$$

and estimated dynamics is proposed

$$\hat{F} = Y(q_a, \dot{q}_a, q_d, \dot{q}_d, \ddot{q}_d)\hat{\theta} + Y_f(l)\hat{\theta}_f \qquad (6.40)$$

, hat ^ means estimation.

Then, the liberalized dynamic of entire system in state-space form is given by [3]

$$\begin{aligned} \dot{x} &= Ax + BF \\ l &= Cx \end{aligned} \qquad (6.41)$$

where x is state variable $x = \begin{bmatrix} l & \dot{l} \end{bmatrix}^T$.

As a result, the error of joint is defined as difference between estimated length and real length

$$e = x - \hat{x} \qquad (6.42)$$

And the estimated parameter error is given by

$$\phi = \theta - \hat{\theta} \quad , \quad \phi_f = \theta_f - \hat{\theta}_f \qquad (6.43)$$

Afterward, introduce estimated error to dynamic equation

$$\begin{aligned} \dot{e} &= Ae + B\tilde{F} \\ E &= Ce \end{aligned} \qquad (6.44)$$

where E is trajectory error and $\tilde{F} = F - \hat{F} = Y\phi + Y_f\phi_f$.

The positive definite and diagonal matrices P, M are available

$$\begin{aligned} A^T P + PA &= -Q \\ PB &= C \end{aligned} \qquad (6.45)$$

For deriving adaptation law, a Lyapunov candidate function is chosen

$$V(e, \phi, \phi_f) = \frac{1}{2}\left(e^T Pe + \phi^T \Gamma^{-1}\phi + \phi_f^T \Gamma_f^{-1}\phi_f\right) \qquad (6.46)$$

Then, differentiation to time leads the candidate function to

$$\begin{aligned} \dot{V} &= \dot{e}^T Pe + \dot{\phi}^T \Gamma^{-1}\phi + \dot{\phi}_f^T \Gamma_f^{-1}\phi_f \\ &= e^T\left(A^T P + PA\right)e + C\tilde{F}^T e + \dot{\phi}^T \Gamma^{-1}\phi + \dot{\phi}_f^T \Gamma_f^{-1}\phi_f \\ &= -e^T Qe + \left(Y^T E + \dot{\phi}^T \Gamma^{-1}\right)\phi + \left(Y_f^T E + \dot{\phi}_f^T \Gamma_f^{-1}\right)\phi_f \end{aligned} \qquad (6.47)$$

where Γ, Γ_f are positive definite and diagonal matrices.

For guaranteeing stability of system, the differential should be smaller than zero. Consequently, adaptation law is set

$$\dot{\phi} = -\Gamma Y^T E \ , \ \dot{\phi}_f = -\Gamma_f Y_f^{\ T} E \tag{6.48}$$

, and the differential Lyapunov function is obtained in negative form

$$\dot{V} = -\dot{e}^T Q e \le 0 \tag{6.49}$$

which guarantees the system globally stable, and deviation of parameter $\wp$ and

trajectory error e to go to zero. Since $\phi = \theta - \hat{\theta}$, $\phi_f = \theta_f - \hat{\theta}_f$, the $\dot{\hat{\theta}} = \dot{\phi}$, $\dot{\hat{\theta}}_f = \dot{\phi}_f$ and

adaptive rule for adapting parameter vector with updating by time

$$\dot{\hat{\theta}} = -\Gamma Y^T E \ , \ \dot{\hat{\theta}}_f = -\Gamma_f Y_f^{\ T} E \tag{6.50}$$

With dynamic model, the robot system can be controlled more precisely and rapidly. It needs available computational model and resolve subtle deviation of model occurred by external disturbance. On the other hand, adaptive controlling law helps us modifying the systemic parameters and improving control effectiveness. Thus, implementing the MCCPM system in the dynamic control system will validate the hydraulic manipulator well performing in trajectory tracking. The structure of hydraulic manipulator system with adaptive controller and MCCPM system is shown in Fig. 6.4.
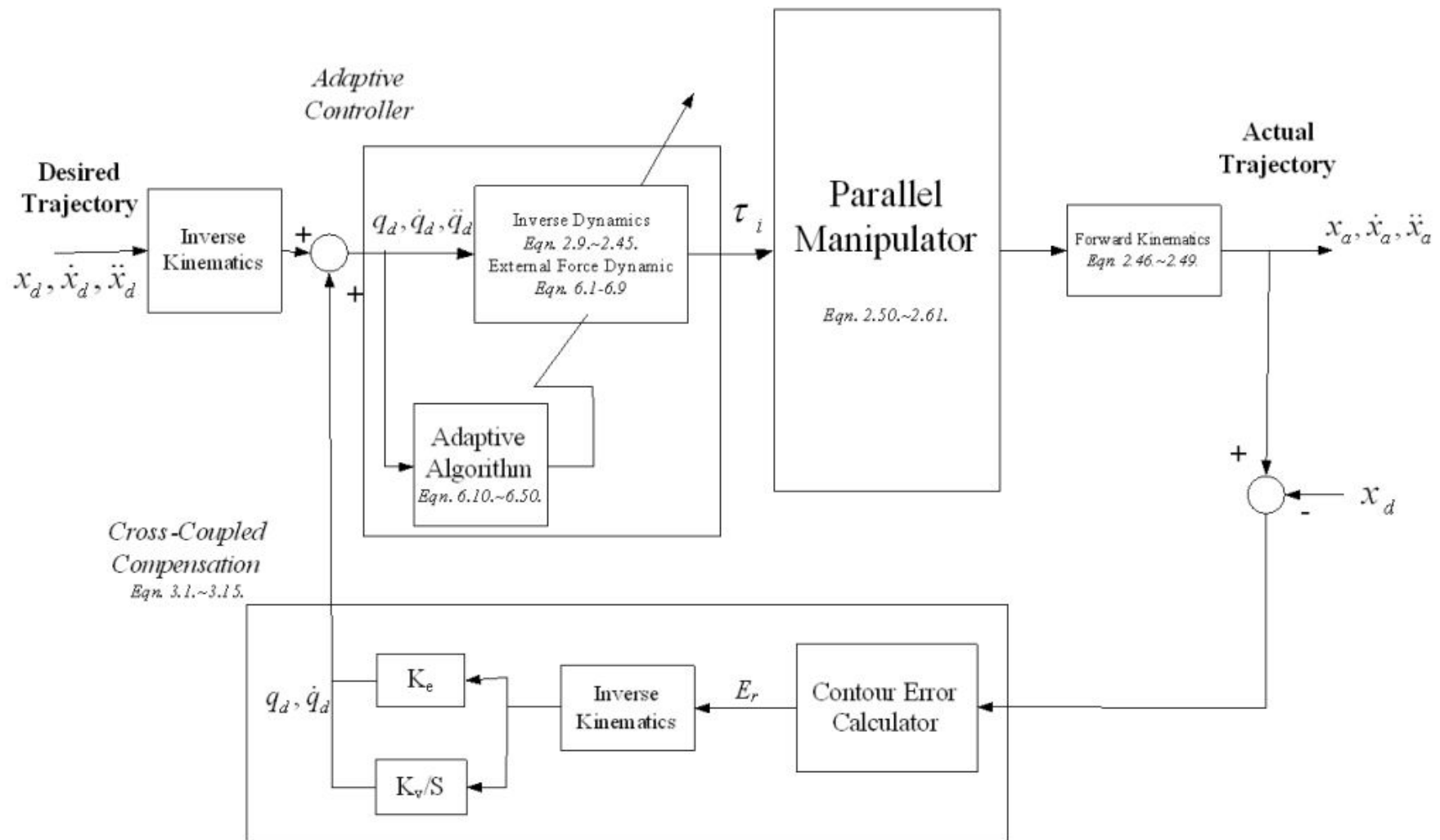
Fig. 6.4. Control flow chart with adaptive control and MCCPM system

REFERENCES

[1] C. Canudas de Wit, Olsson H., K.J. Astrom, and P. Lischinsky, "A new model for control of systems with friction," *IEEE, Trans. Automat. Contr.*, Vol. 40, No. 3, Mar. 1995, pp. 419-425.

[2] Zheng Li, Y. S. Chiou, and Steven Y. Liang, "Three dimensional cutting force analysis in end milling," *Int. J. Mech. Sci.*, Vol. 38, No. 3, 1996, pp. 259-269.

[3] P. Lischinsky, C. Canudas-de-Wit, and G. Morel, "Friction compensation for an industrial hydraulic robot," *Control Systems Mag, IEEE*, Vol. 19, Issue 1, Feb. 1999 pp. 25 – 32.

[4] Herbert E. Merrit. "Hydraulic control systems," *John Wiley & Sons, Inc.,* 1967

[5] J. Zhou, "Experimental Evaluations of a Kinematic compensation control method for hydraulic robot manipulators," *Control Eng. Practice*, Vol. 3, No. 5, 1995, pp. 675-684.

[6] K. Kosuge, K. Takeo, T. Fukuda, H. Kitayama, N. Takeuchi, and H. Murakami, "Force control of parallel link manipulator with hydraulic actuators," *Int. Conf. Robotics and Automation*, 1996, pp. 305-310.

[7] Yuan-Ming Cheng, Jih-Hua Chin, "Machining contour errors as ensembles of cutting, feeding and machine structure effects," *Int. J. Mach. Tools Manuf.* 43 (2003), pp. 1001-1014.

[8] 陳昱丞, "基因演算法對複合式運動平台協同運動之最佳化," *Dep. Mech. Eng. NCTU, Taiwan, ROC.*, Master Thesis, 2004.

[9] Jih-Hua Chin, Her-Chyi Tsai, "A path algorithm for robotic machining," *Robotics & Computer-Integrated Manuf,* Vol. 10, No. 3, 1993, pp. 195-198.

[10] Chih-Wei Lue, Yuan-Ming Cheng, and Jih-Hua Chin "System structure and contour tracking for a hybrid motion platform", *Int. J. Adv. Manuf. Tech.*, DOI. 10.1007/s00170-004-211-2., 2004

[11] Honegger, M., "Adaptive control of the Hexaglide, a 6 DOF parallel manipulator," *Proc. IEEE ICRA,* Albuquerque NM,USA, 1997.

[12] Rolf Johansson, "Adaptive control of robot manipulator motion," *IEEE Trans. on robotics and automation,* Vol. 6, No. 4, Aug. 1990, pp. 483-490.

[13] Michael W. Walker, Liang-Boon Wee, "An adaptive control strategy for space based robot manipulators," *Proc. IEEE ICRA,* Sacramento CA, USA, Apr. 1991.

[14] A. Benallegue, "Adaptive control for flexible-joint robots using a passive systems approach," *Control Eng. Practice,* Vol. 3, No. 10,   1995, pp.1393-1400.

[15] Gang Feng, "A new adaptive control algorithm for robot manipulators in task space," *IEEE Trans. on robotics and automation,* Vol. 11, No. 3, Jun. 1990, pp. 457-462.

[16] B. Dasgupta$_a$, T.S. Mruthyunjaya, "The Stewart platform manipulator: a review," *Mech. Mach. Theory,* Vol. 35, No.1, 2000, pp. 15-40.

[17] Geng, Z., Haynes, L. S., Lee, J. D. and Carroll, R. L., "On the dynamic model and kinematics analysis of a class of Stewart platforms," *Robotics and Autonomous Syst.* 9, 1992, pp. 237-254.

[18] Lung-Wen Tsai, "Robot analysis – The mechanics of serial and parallel manipulators," *Wiley & Sons, Inc.*, 1999.

[19] Lung-Wen Tsai, "Solving the inverse dynamics of a Stewart-Gough manipulator by the principle of virtual work," *J. of Mechanical Design, ASME,* Vol. 122, Mar. 2000, pp. 3-9.

[20] B. Dasgupta, T. S.Mruthyunjaya, "A Newton-Euler formulation for the inverse dynamics of the Stewart platform manipulator," *Mech. Mach. Theory,* Vol. 33, No. 8, 1998, pp. 1135-1152.

[21] K. Harib, K Srinivasan., "Kinematic and dynamic analysis of Stewart platform-based machine tool structures," *Robotica*, Vol. 21, 2003, pp. 541-554.

[22] B. Dasgupta, T. S. Mruthyunjaya, "Closed-form dynamic equations of the general Stewart platform through the Newton-Euler approach," *Mech. Mach. Theory,* Vol. 33, No. 7, 1998, pp. 993-1012.

[23] Jih-Hua Chin, Xiang-En Peng, 2004, "A tracking simulation for a hybrid Stewart platform manipulator", *Proc. IASTED International Conf. on Modelling and Simulation,* Cancun, Mexico, May 18-21, 2005.

[24] L. Sciavicco, B. Siliano, "Modeling and control of robot manipulators," *McGraw-Hill, Inc.,* 1996.

[25] G. P. Liu, S. Daley, "Optimal-tuning nonlinear PID control of hydraulic systems," *Control Eng. Practice*, Vol. 8, 2000, pp. 1045-1053.

[26] M. R. Sirouspour, S. E. Salcudean, "Nonlinear control of a hydraulic parallel manipulator," *IEEE Trans. Robotics and Automation*, vol. 17, no. 2, Apr. 2001, pp. 173-182.

[27] Jih-Hua Chin, H. W. Lin, "The algorithms of the cross-coupled pre-compensation method for generation the involute-type scrolls," *ASME J. Dynamic Systems, Measurement, and Control*, March, Vol.121, 1999, pp.96-104.

[28] Kunwoo Lee, "Principles of CAD/CAM/CAE system," *Addison Wesley*, 1999

[29] B. Siciliano, L. Villani, "Adaptive compliant control of robot manipulators," *Control Eng. Practice*, Vol. 4, No. 5, 1996, pp. 705-712.

[30] F. Alonge, F. D'Ippolito, F.M. Raimondi, "Globally convergent adaptive and robust control of robotic manipulators for trajectory tracking," *Control Eng. Practice*, Vol. 12, Apr. 2004, pp. 1091-1100.

[31] Lung-Wen Tsai, "Solving the inverse dynamics of a Stewart-Gough manipulator by the principle of virtual work," *J. of Mechanical Design, ASME,* Vol. 122, Mar. 2000, pp. 3-9.

[32] J. Tlusty, "Dynamics of cutting forces in end milling," *Annals of the CIRP*, Vol. 24, No. 1, 1975, pp. 433-436.

[33] M. Y. Yang, T. M. Lee, "Hybrid adaptive control based on the characteristics of CNC end milling," *Int. J. Mach. Tools Manuf.*, Vol. 42, 2002, pp. 489-499.

[34] T. Y. Kim, J. W. Kim, "Adaptive cutting force control for a machining center by using indirect cutting force measurements," *Int. J. Mach. Tools Manuf.*, Vol. 36, No. 8, 1996, pp. 925-937.

[35] D. S. Kwon, S. M. Babcock, and *et al,* "Tracking control on the hydraulically actuated flexible manipulator," *IEEE Int. Conf. on Robotics and Automation,* vol.3, 1995, pp 2200 – 2205.

簡介

姓名：孫晏晞　(Sun, Yen-Hsi)

生日：1981 年 11 月 5 日

學歷：

高雄市立小港國小	1988.9 – 1994.6
高雄市立小港國中	1994.9 – 1997.6
高雄市私立道明中學	1997.9 – 2000.6
國立交通大學機械工程系學士班	2000.9 – 2004.1
國立交通大學機械工程系碩士班	2004.2 – 2005.6

通訊錄：高雄市小港區中船二村十七號　07-831-4850

E-Mail: yancsun@gmail.com

Vita

Full Name: Sun, Yen-His

Date of Birth: 1981/11/05

Educational Background:

Kaohsiung Hsiao-Kang Elementary School	1988.9 – 1994.6
Kaohsiung Hsiao-Kang Senior High School	1994.9 – 1997.6
St. Dominic High School	1997.9 – 2000.6
National ChiaoTung University -	2000.9 – 2004.1
Department of Mechanical Engineering	2004.2 – 2005.6

Address: No.17, Jhong-Chuan 2nd Village, Siaogang District

Kaohsiung, 812, Taiwan (R.O.C)　886-7-8314850

E-Mail: yancsun@gmail.com